



Synthesis, DFT calculation, pharmacological evaluation, and catalytic application in the synthesis of diverse pyrano[2,3-*c*]pyrazole derivatives

Mostafa M.K. Amer^a, Magda H. Abdellattif^b, Samar M. Mouneir^c, Wael A. Zordok^a,
Wesam S. Shehab^{a,*}

^a Department of Chemistry, Faculty of Science, Zagazig University, Zagazig 44519, Egypt

^b Department of Chemistry, College of Science, Taif University, Taif 21944, Saudi Arabia

^c Department of Pharmacology, Faculty of Veterinary Medicine, Cairo University, Cairo 12211, Egypt

ARTICLE INFO

Keywords:

Multicomponent reaction
Pyrano[2,3-*c*]pyrazole
DFT/B3LYP
HOMO - LUMO
Anti-inflammatory
Antioxidant

ABSTRACT

Pyranopyrazole and its derivatives are classified to be a pharmacologically significant active scaffold for almost all modes of biological activities. In this work, An efficient, green, and facile three-component reaction for preparing pyrano[2,3-*c*]pyrazole derivatives via the condensation reaction of 5-methyl-2,4-dihydro-3H-pyrazol-3-one, ethyl acetoacetate, and malononitrile in the presence of ZnO Nanoparticle. The products are produced with high yields and in shorter reaction times. It also is mild, safe, green, and environmentally friendly. The geometric parameters such as dipole moment, bond length, dihedral angles, total energy, heat of formation, atomic charges and energies at a highly accurate for prepared compounds were computed by Density Functional Theory along with the B3LYP functional. The newly synthesized compounds were screened for their anti-inflammatory and antioxidant activity. Some of the tested compounds displayed promising activities. The newly prepared compounds were found to be potent towards the antioxidant activity. Results indicated that compounds **11** and **12** exhibited significant ($p \geq 0.05$) in vitro total antioxidant activity as 44.93 ± 0.15 and 39.60 ± 0.10 U/ML, respectively higher than standard ascorbic acid (29.40 ± 0.62).

1. Introduction

Pollution is a significant universal problem today, so one of the exciting challenges for synthetic organic chemists is designing organic reactions following eco-friendly and straightforward protocol. Green and simple synthetic protocols are vital concerns in organic synthesis since then, multicomponent reactions (MCRs) have identified as a valuable synthetic approach in organic, medicinal, and combinatorial chemistry research [1,2] because of ensuring high atom economy, shorter reaction times, good overall yields, and high chemo and regioselectivity as well as minimizing waste and avoidance of expensive purification processes [3]. It has been recognized that MCRs are much more eco-friendly and offer rapid access to the structural diversity of resulting compounds when compared to conventional multistep synthesis [4].

Metal oxide nanoparticles as nanocatalysts have emerged as promising heterogeneous catalysts for various organic transformations because of affording high surface area to volume ratio in the reaction,

which improves their efficacy, selectivity, and catalytic activity [5]. Recently, nano-ZnO has great utilization as an efficient heterogeneous catalyst in organic synthesis of varied biologically active heterocycles due to its cheap cost, non-toxicity, commercial availability, environmental friendliness, efficient high reactivity, and reusability benefits [6].

Pyrano[2,3-*c*]pyrazole motifs are a privileged structure in several bioactive heterocyclic scaffolds possessing potential pharmacological effects [7,8] such as compound **A** acting as human Chk1 kinase inhibitors [9], **B** as an antimicrobial agent [10], and **C** as a molluscicidal agent [11] (Fig. 1) besides anti-inflammatory [12], anti-bacterial [13], antifungal [14,15], antimalarial [16], antiproliferative [17], anti-cancer [18], anti-depressant [19], antioxidant [20], α -glucosidase inhibitors [21], and analgesic [22] activities. Also, pyrano[2,3-*c*]pyrazole frameworks have been demonstrated to exhibit enormous application in biodegradable agrochemicals [23-25] and treating Alzheimer's diseases [26,27]. Additionally, annulated pyranopyrazole systems have a broad spectrum of biological activities, including pyrazolopyranopyrimidine

* Corresponding author.

E-mail address: Dr.wesamshehab@gmail.com (W.S. Shehab).

<https://doi.org/10.1016/j.bioorg.2021.105136>

Received 11 June 2021; Accepted 27 June 2021

Available online 1 July 2021

0045-2068/© 2021 Elsevier Inc. All rights reserved.

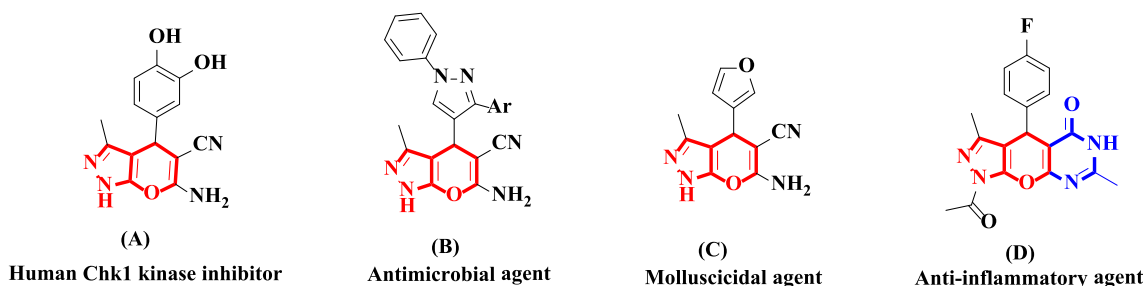


Fig. 1. Examples of Pyrano[2,3-c]pyrazoles with reported human Chk1 kinase inhibitors (A), antimicrobial (B) and Molluscicidal (C) activities, and pyrazolopyranopyrimidine derivative (D) with reported anti-inflammatory activity.

building block in compound **D** as an anti-inflammatory agent [28] (Fig. 1).

Inflammation is a part of the complex biological response of vascular tissues to harmful stimuli, such as pathogens, damaged cells, or irritants. It can be acute or chronic; acute inflammation is rapid in onset and of short period, lasting from a few minutes to as long as few days, and is characterized by fluid and plasma protein exudation, whereas chronic inflammation is of longer duration, typified by the influx of lymphocytes and macrophages with associated vascular proliferation and fibrosis [29].

Motivated by the aforementioned subjects and continuing our efforts in the field of nanocatalysts and synthesis of bioactive heterocycles [30–35], we wish to report nano-ZnO as an efficient catalyst for green and facile one-pot three-component reaction of 5-methyl-2-phenyl-2,4-dihydro-3H-pyrazol-3-one, thiophene-2-carbaldehyde, and malononitrile to produce 6-amino-3-methyl-1-phenyl-4-(thiophen-2-yl)-1,4-dihydropyrano[2,3-c]pyrazole-5-carbonitrile furthermore our research prolonged to the synthesis of pyrazolopyranopyrimidine analogs with theoretical investigation using DFT calculations and assessed them in vitro as anti-inflammatory agents compared to the most widely used NSAIDs celecoxib and quercetin besides evaluating their in vitro antioxidant activity compared to standard ascorbic acid.

2. Experimental section

2.1. Materials and methods

All chemicals were purchased from Sigma-Aldrich (Taufkirchen, Germany), and all solvents were purchased from El-Nasr Pharmaceutical Chemicals Company (analytical reagent grade, Egypt). Thiophene-2-carbaldehyde was purchased from the Central Laboratory of Health Ministry. All chemicals were used as supplied without further purification. The melting points were measured by a digital Electrothermal IA 9100 Series apparatus Cole-Parmer, Beacon Road, Stone, Staffordshire, ST15 OSA, UK) and were uncorrected. C, H, and N analyses were carried out on a PerkinElmer CHN 2400. IR spectra were recorded on FT-IR 460 PLUS (KBr disks) in the range from 4000 to 400 cm^{-1} . ^1H and ^{13}C NMR spectra were recorded on a Bruker 400 MHz NMR Spectrometer using tetramethylsilane (TMS) as the internal standard, chemical shifts are expressed in δ (ppm), and DMSO- d_6 was used as the solvent. The mass spectrum was carried out on the direct probe controller inlet part to a single quadrupole mass analyzer in the thermo scientific GCMS model (ISQLT) using thermo X-Calibur software. At the Regional Centre for Mycology & Biotechnology (RCMB) Al-Azhar University, Naser City, Cairo.

2.2. Synthesis

2.2.1. Synthesis of 6-amino-3-methyl-1-phenyl-4-(thiophen-2-yl)-1,4-dihydropyrano[2,3-c]pyrazole-5-carbonitrile (**1**)

A mixture of 5-methyl-2-phenyl-2,4-dihydro-3H-pyrazol-3-one (1 g, 0.005 mol), thiophene-2-carbaldehyde (0.64 g, 0.53 mL, 0.005 mol) and

malononitrile (0.37 g, 0.31 mL, 0.005 mol) in ethanol (10 mL), in the presence of a catalytic amount of supported metal nanoparticle ZnO (0.08 g, 0.0009 mol) was refluxed for 2 h. After reaction completion, the solid product was collected by filtration, washed with ethanol, and crystallized from ethanol to afford compound **1** as pale-yellow crystals: 85%, mp: 178–180 °C. IR (KBr, ν , cm^{-1}): 3456, 3312 (NH_2), 2210 (CN), 1656 ($\text{C}=\text{N}$), 1586 (Ar) cm^{-1} ; ^1H NMR (DMSO- d_6 , 400 MHz): δ = 2.25 (s, 3H, CH_3), 5.42 (s, H, CH methine), 6.92 (d, H, H-5thiophene), 6.94 (d, H, H-3thiophene), 6.91–7.07 (m, 5H, ArH's), 7.34 (2H, s, NH_2); ^{13}C (125 MHz, DMSO- d_6): 160.20 (C6), 146.82, 144.74, 143.87, 183.40, 132.45, 130.60, 130.19, 129.36, 127.10, 120.97, 120.73, 115.62 (CN), 58.82 (C5), 39.90 (C4), 9.73, 21.56, 14.51. Anal. calcd. For $\text{C}_{18}\text{H}_{14}\text{N}_4\text{OS}$ (334.09): C, 64.65; H, 4.22; N, 16.75; S, 9.59%. Found: C, 64.69; H, 4.20; N, 16.74; S, 9.57%.

2.2.2. Synthesis of 3-methyl-1-phenyl-4-(thiophen-2-yl)-1,4-dihydropyrazolo[4',3':5,6]pyrano[2,3-d]pyrimidin-5-amine (**2**)

A mixture of compound **1** (0.5 g, 0.001 mol) and formamide (20 mL) was refluxed for 3 h. After reaction completion, the reaction mixture was cooled and poured over ice cold water. The formed solid was filtered off, dried and recrystallized from ethanol to yield compound **2** as a gray solid: 86.6%, mp: 250–252 °C. IR (KBr, ν , cm^{-1}): 3456, 3312 (NH_2), 1656 ($\text{C}=\text{N}$), 1586 (Ar) cm^{-1} ; ^1H NMR (DMSO- d_6 , 400 MHz): δ = 1.93 (s, 3H, CH_3), 5.42 (s, H, CH pyrane), 6.92 (d, H, H-5thiophene), 6.94 (d, H, H-3thiophene), 6.91–7.07 (m, 5H, ArH's), 7.44 (s, 2H, NH_2) ppm. Anal. calcd. For $\text{C}_{19}\text{H}_{15}\text{N}_5\text{OS}$ (361.10): C, 63.14; H, 4.18; N, 19.38; S, 8.87%. Found: C, 63.14; H, 4.19; N, 19.39; S, 8.86%.

2.2.3. Synthesis of 3-methyl-1-phenyl-4-(thiophen-2-yl)-4,6-dihydropyrazolo[4',3':5,6]pyrano[2,3-d]pyrimidin-5(1H)-one (**3**)

A mixture of compound **1** (0.5 g, 0.001 mol) and formic acid (20 mL) was heated under reflux conditions for 8 h. After reaction completion, the reaction mixture was cooled and poured over ice cold water. The formed solid was filtered off, dried and recrystallized from ethanol to give compound **3** as a greenish solid: 73%, mp: 260–262 °C. IR (KBr, ν , cm^{-1}): 3350–3550 (NH stretch), 3103 (aromatic CH), 1649 ($\text{C}=\text{O}$ amide), 1598 ($\text{C}=\text{N}$), 1071 ($\text{C}-\text{S}$ stretch). ^1H NMR (DMSO- d_6 , 400 MHz) δ = 2.49 (s, 3H, CH_3), 6.92 (d, H, H-5thiophene), 6.94 (d, H, H-3thiophene), 6.91–7.37 (m, 5H, ArH's), 12.16 (s, H, NH exchangeable by D_2O) ppm. ^{13}C (125 MHz, DMSO- d_6): 162.31 ($\text{C}=\text{O}$), 152.68 ($\text{C}=\text{N}$), 149.16, 139.01, 134.52, 134.06, 133.78, 129.71, 129.51, 127.58, 125.49, 119.24, 13.98; MS, m/z (%): 362 (M^+ , 30). Anal. calcd. For $\text{C}_{19}\text{H}_{14}\text{N}_4\text{O}_2\text{S}$ (362.08): C, 62.97; H, 3.89; N, 15.46; O, 8.83; S, 8.85%. Found: C, 63.14; H, 4.19; N, 19.39; S, 8.86%.

2.2.4. Synthesis of 7-(chloromethyl)-3-methyl-1-phenyl-4-(thiophen-2-yl)-4,6-dihydropyrazolo[4',3':5,6]pyrano[2,3-d]pyrimidin-5(1H)-one (**4**)

A mixture of **1** (0.5 g, 0.001 mol) and chloroacetyl chloride (0.112 g, 0.08 mL, 0.001 mol) in DMF (5 mL) was refluxed for 10 h. After reaction completion, the reaction mixture was cooled and poured over ice cold water, and the precipitate formed was filtered and crystallized from ethanol to produce compound **4** as brown crystals: 25%, mp:

318–320 °C. IR (KBr, ν , cm^{-1}). 3350–3550(NH stretch), 3103 (aromatic CH), 1649 (C=O amide), 1598 (C=N), 1071 (C–S stretch). ^1H NMR (DMSO- d_6 , 400 MHz) δ = 2.25 (s, 3H, CH_3), 4.22(s, 2H, CH_2), 5.23(s, 1H, CH, pyrane) 6.92 (d, H, H-5thiophene), 6.94 (d, H, H-3thiophene), 6.91–7.37 (m, 5H, ArH's), 12.16 (s, H, NH exchangeable by D_2O) ppm. ^{13}C (125 MHz, DMSO- d_6): 162.20, 146.82, 144.74, 143.87, 183.40, 132.45, 130.60, 130.19, 129.36, 127.10, 120.97, 120.73, 98.64, 58.82, 39.90, 22.56, 19.24. Anal. calcd. For $\text{C}_{20}\text{H}_{15}\text{ClN}_4\text{O}_2\text{S}$ (410.06): C, 58.47; H, 3.68; N, 13.64; S, 7.80%. Found: C, 58.44; H, 3.67; N, 13.64; S, 7.79%.

2.2.5. Synthesis of 5-amino-3-methyl-1-phenyl-4-(thiophen-2-yl)-1,4-dihydropyrazolo[4',3':5,6]pyrano[2,3-d]pyrimidine-7-thiol (5)

A mixture of compound 1 (0.5 g, 0.001 mol) and thiourea (0.08 g, 0.001 mol) was fused under dry conditions in oil bath for 0.5 h, the fused mixture was dissolved in ethanol (10 mL) and the resulting solution was refluxed for 3 h in the presence of few drops of piperidine. After reaction completion, the reaction mixture was cooled and the precipitate formed was collected by filtration and the filtrate further worked up by diluting with cold water to give additional amount of the product which was washed with ethanol, dried, and recrystallized from ethanol to provide compound 4 as red crystals: 45%, mp: over 360 °C. IR (KBr, ν , cm^{-1}) 0.3389 (NH_2), 3103 (aromatic CH), 1598 (C=N), 1071 (C–S stretch). ^1H NMR (DMSO- d_6 , 400 MHz) δ = 2.25 (s, 3H, CH_3), 5.60 (s, 1H, CH purine), 6.92 (d, H, H-5thiophene), 6.94 (d, H, H-3thiophene), 6.91–7.56 (m, 5H, ArH's), 7.93 (s, 1H, $\text{D}_2\text{OExch.NH}_2$), 12.16 (s, H, $\text{D}_2\text{OExch.SH}$) ppm. ^{13}C (125 MHz, DMSO- d_6): 175.30, 173.82, 153.74, 152.45, 150.87, 143.40, 133.45, 130.70, 129.36, 127.10, 120.97, 120.73, 98.64, 58.82, 39.90, 22.56, 13.32. Anal. calcd. For $\text{C}_{19}\text{H}_{15}\text{N}_5\text{OS}_2$ (393.07): C, 58.00; H, 3.84; N, 17.80; S, 16.30%. Found: C, 58.04; H, 3.84; N, 17.81; S, 16.30%.

2.2.6. Synthesis of ethyl 5-amino-3-methyl-1-phenyl-4-(thiophen-2-yl)-4,7-dihydro-1H-pyrrolo[3',2':5,6]pyrano[2,3-c]pyrazole-6-carboxylate (6)

A mixture of compound 1 (0.5 g, 0.001 mol), ethyl chloroacetate (0.25 g, 0.21 mL, 0.002 mol) and anhydrous K_2CO_3 (0.13 g, 0.001 mol) in dry acetone (10 mL) was stirred under reflux for 10 h. The reaction mixture was left overnight then poured over crushed ice. The formed precipitate was filtered off, washed with water, dried, and crystallized from ethanol to furnish compound 6 as dark red crystals: 70%, mp: 230–232 °C. IR (KBr, ν , cm^{-1}). 3397 (NH), 3389 (NH_2), 1705 (C=O ester). ^1H NMR (DMSO- d_6 , 400 MHz) δ = 1.2(t, 3H, CH_3), 2.5(s, 3H, CH_3), 4.2(q, 2H, CH_2), 5.60 (s, 1H, CH purine), 6.92 (d, H, H-5thiophene), 6.94 (d, H, H-3thiophene), 6.91–7.56 (m, 5H, ArH's), 7.93 (s, 1H, NH_2), 11.90 (s, 1H, NH), ppm. ^{13}C (125 MHz, DMSO- d_6): 165.20, 156.90, 153.74, 152.45, 150.87, 143.40, 133.45, 130.70, 129.36, 127.10, 120.97, 120.73, 98.64, 58.82, 45.78 39.90, 22.56, 13.32. Anal. calcd. For $\text{C}_{22}\text{H}_{20}\text{N}_4\text{O}_3\text{S}$ (420.13): C, 62.84; H, 4.79; N, 13.32; S, 7.62%. Found: C, 62.83; H, 4.80; N, 13.30; S, 7.60%.

2.2.7. Synthesis of 3-methyl-7-(4-nitrophenyl)-1-phenyl-4-(thiophen-2-yl)-4,6,7,8-tetrahydropyrazolo[4',3':5,6]pyrano[2,3-d]pyrimidin-5(1H)-one (7)

A mixture of compound 1 (0.5 g, 0.001 mol) triturated with ethanol, *p*-nitrobenzaldehyde (0.15 g, 0.001 mol), and few drops of piperidine was fused in oil bath for 1.5 h and the reaction mixture was left to cool then the resulting solid was dissolved in ethanol. The resulting solution was diluted with crushed ice acidified with HCl then the formed precipitate was collected by filtration, dried, and recrystallized from ethanol to give compound 7 as dark brown crystals: 93%, mp: 256–258 °C. IR (KBr, ν , cm^{-1}). 3350–3550(NH stretch), 3103 (aromatic CH), and 1649 (C=O amidic). ^1H NMR (DMSO- d_6 , 400 MHz) δ = 1.92(s, 3H, CH_3), 5.45(s, 1H, CH), 6.92 (d, H, H-5thiophene), 6.94 (d, H, H-3thiophene), 6.91–8.56 (m, 10H, ArH's), 9.87 (s, 1H, NH) ppm. ^{13}C (125 MHz, DMSO- d_6): 167.33, 162.86, 153.74, 152.45, 145.87, 143.40, 133.45, 130.70, 129.36, 125.40, 126.84, 127.10, 122.54, 121.42, 120.97, 120.73, 115.79, 98.64, 58.82, 45.78. Anal. calcd. For $\text{C}_{25}\text{H}_{19}\text{N}_5\text{O}_4\text{S}$

(485.12): C, 61.85; H, 3.94; N, 14.42; S, 6.60%. Found: C, 61.83; H, 3.93; N, 14.41; S, 6.59%.

2.2.8. Synthesis of 5-amino-3-methyl-1-phenyl-4-(thiophen-2-yl)-4,8-dihydropyrazolo[4',3':5,6]pyrano[2,3-b]pyridin-7(1H)-one (8)

A mixture of compound 1 (0.5 g, 0.001 mol), ethyl cyanoacetate (0.113 g, 0.10 mL, 0.001 mol), ammonium acetate (0.07 g, 0.001 mol), and glacial AcOH (5 mL) was heated under reflux for 2 h then cooled and poured over crushed ice. The formed solid was collected by filtration and recrystallized from ethanol to produce compound 8 as brown crystals: 53%, mp 240–242 °C. IR (KBr, ν , cm^{-1}). 3446, 3320 (NH, NH_2) and 1650 (C=O). ^1H NMR (DMSO- d_6 , 400 MHz) δ = 1.95(s, 3H, CH_3), 4.95 (s, 1H, CH), 6.92 (d, H, H-5thiophene), 6.94 (d, H, H-3thiophene), 6.91–8.56 (m, 5H, ArH's), 8.89 (s, 2H, NH_2), 11.30(s, 1H, NH) ppm. ^{13}C (125 MHz, DMSO- d_6): 163.30, 160.86, 152.74, 150.40, 145.87, 140.39, 133.45, 130.70, 129.36, 129.00, 126.38, 125.10, 124.54, 121.42, 120.97, 120.73, 115.79, 98.64, 58.82, 45.78. Anal. calcd. For $\text{C}_{20}\text{H}_{16}\text{N}_4\text{O}_2\text{S}$ (376.10): C, 63.81; H, 4.28; N, 14.88; S, 8.52%. Found: C, 63.82; H, 4.28; N, 14.80; S, 8.51%.

2.2.9. Synthesis of 5-chloro-3-methyl-1-phenyl-4-(thiophen-2-yl)-1,4-dihydropyrazolo[4',3':5,6]pyrano[2,3-d]pyrimidine (9)

To a cold solution of compound 1 (0.5 g, 0.001 mol) in conc. HCl (2 mL), a solution of sodium nitrite (0.06 g, 0.001 mol) in 5 mL water was added with stirring in ice bath (at 5 °C). After the completion of sodium nitrite solution addition, the product was separated, collected by filtration, and recrystallized from ethanol to provide compound 9 as reddish brown crystals: 35%, mp 298–300 °C. IR (KBr, ν , cm^{-1}). 3103 (aromatic CH), 1598 (C=N), 1071 (C–S stretch). ^1H NMR (DMSO- d_6 , 400 MHz) δ = 2.49 (s, 3H, CH_3), 6.92 (d, H, H-5thiophene), 6.94 (d, H, H-3thiophene), 6.91–7.37 (m, 5H, ArH's) ppm. MS, m/z (%): 380.8 (M^+ , 30). Anal. calcd. For $\text{C}_{19}\text{H}_{13}\text{ClN}_4\text{OS}$ (380.85): C, 59.92; H, 3.44; N, 14.71; S, 8.42%. Found: C, 59.91; H, 3.44; N, 14.70; S, 8.41%.

2.2.10. Synthesis of 7-amino-3-methyl-5-oxo-1-phenyl-4-(thiophen-2-yl)-1,4,5,8-tetrahydropyrazolo[4',3':5,6]pyrano[2,3-b]pyridine-6-carbonitrile (10)

A mixture of compound 1 (0.5 g, 0.001 mol), malononitrile (0.06 g, 0.001 mol) and few drops of piperidine in DMF was refluxed for 12 h, the mixture was allowed to cool down to room temperature, poured over crushed ice acidified with HCl, the formed precipitate was collected by filtration, dried, and recrystallized from ethanol to yield compound 10 as gray crystals: 20%, mp 284–286 °C. IR (KBr, ν , cm^{-1}). 3446, 3320 (NH, NH_2), 3103 (aromatic CH), and 1650 (C=O). and 1598 (C=N). ^1H NMR (DMSO- d_6 , 400 MHz) δ = 2.20(s, 3H, CH_3), 4.95(s, 1H, CH), 6.92 (d, H, H-5thiophene), 6.94 (d, H, H-3thiophene), 6.91–8.56 (m, 5H, ArH's), 8.89 (s, 2H, NH_2), 12.18 (s, 1H, NH) ppm. Anal. calcd. For $\text{C}_{21}\text{H}_{15}\text{N}_5\text{O}_2\text{S}$ (401.44): C, 62.83; H, 3.77; N, 17.45; S, 7.99%. Found: C, 62.82; H, 3.79; N, 17.46; S, 7.98%.

2.2.11. Synthesis of 3-methyl-6-(((2R,3S,4S,5R,6R)-2,3,4,5,6-pentahydroxytetrahydro-2H-pyran-2-yl)methyl)amino-1-phenyl-4-(thiophen-2-yl)-1,4-dihydropyrano[2,3-c]pyrazole-5-carbonitrile (11)

A mixture of compound 1 (0.5 g, 0.001 mol) and glucose (0.26 g, 0.001 mol) in *tert*-butanol (15 mL) was refluxed for 5 h. After cooling, the formed solid was filtered off, dried, and crystallized from ethanol to furnish compound 11 as red crystals: 50%, mp: 160–162 °C. IR (KBr, ν , cm^{-1}): 3414 cm^{-1} (NH), 3350–3560 cm^{-1} (broad band for OH), 2916 cm^{-1} (CH aliphatic), 2210 cm^{-1} (CN) and 1593 cm^{-1} (C=O for amide). ^1H NMR (DMSO- d_6 , 400 MHz): δ = 1.91 (s, 1H, CH_3), 3.07–4.30 (m, 4H, 4CH), 3.55 (s, 2H, CH_2), 3.67 (s, 1H, NH), 4.45–6.21 (m, 5H, 5OH), 5.23 (s, 1H, HC-pyrane methine), 7.37–7.45 (m, 5H, ArH), 12.29, 12.62 (s, 2H, NH exchangeable by D_2O). ^{13}C NMR (DMSO- d_6 , 100 MHz): δ = 38.54, 38.75, 38.95, 40.16, 40.37, 40.58, 67.5, 69.3, 71.9, 75.8, 79.85, 86.7, 114.5, 164.5 (C=O), 169.23 ppm. Anal. Calcd. For $\text{C}_{24}\text{H}_{24}\text{N}_4\text{O}_7\text{S}$ (512.14): C, 56.24; H, 4.72; N, 10.93; S, 6.26; Found: C, 56.23; H, 4.71;

N, 10.92; S, 6.28%.

2.2.12. Synthesis of 3-methyl-6-(((2*S*,3*S*,4*S*,5*R*,*E*)-2,3,4,5,6-pentahydroxyhexylidene)amino)-1-phenyl-4-(thiophen-2-yl)-1,4-dihydropyrano[2,3-*c*]pyrazole-5-carbonitrile (**12**)

A mixture of **1** (0.5 g, 0.001 mol) and glucose (0.25 g, 0.001 mol) in acetic acid/water (15/5 mL) was refluxed for 8 h. After cooling, the resulting solution was poured over cold water, the formed solid was filtered off, dried, and crystallized from ethanol to yield compound **12** as dark red crystals: 54%, mp: 148–150 °C. IR (KBr, ν , cm^{-1}): 3350–3500 cm^{-1} (very broad band for OH and absence of NH_2), 3166–2923 cm^{-1} (CH, aromatic and aliphatic) and 2215 cm^{-1} (CN). ^1H NMR (DMSO- d_6 , 400 MHz): δ = 2.21 (s, 1H, CH_3), 3.38–3.82 (m, 4H, 4CH), 3.90 (s, 2H, CH_2), 4.22–5.42 (m, 5H, 5OH), 8.20 (s, 1H, $\text{CH}=\text{N}$), 5.16 (s, 1H, HC-pyrane methine), 7.20–7.82 (m, 5H, ArH), 11.07, 12.28 ppm (s, 2H, 2NH exchangeable by D_2O). ^{13}C NMR (DMSO- d_6 , 100 MHz): δ = 34.54, 36.75, 39.95, 40.16, 40.37, 40.58, 64.5, 65.7, 70.55, 71.42, 73.8, 115.2, 125.7, 164.3 (C=N), 162.4 (C=O), and 170.3 (C=O) ppm. Anal. Calcd. for $\text{C}_{24}\text{H}_{24}\text{N}_4\text{O}_6\text{S}$ (496.14): C, 58.05; H, 4.87; N, 11.28; O, 19.33; S, 6.46; Found: C, 58.05; H, 4.88; N, 11.28; S, 6.45%.

2.3. Computational details

The geometric parameters and energies were computed by density functional theory at the B3LYP/CEP-31G level of theory, using the GAUSSIAN 98W package of the programs [36], on geometries that were optimized at CEP-31G basis set. The high basis set was chosen to detect the energies at a highly accurate level. The atomic charges were computed using the natural atomic orbital populations. The B3LYP is the key word for the hybrid functional [37], which is a linear combination of the gradient functionals proposed by Becke [38] and Lee, Yang and Parr [39], together with the Hartree-Fock local exchange function [40].

2.4. Pharmacology

In-vitro COX-1/ COX-2 inhibitory assay: This assay was investigated using Cayman colorimetric COX (ovine) inhibitor screening assay kit following the manufacturer's instructions compared to standard (Celecoxib) and expressed as μM . **In-vitro 5-LOX inhibitory assay:** This assay was made using a 5-Lipoxygenase Inhibitory screening Assay Kit according to manufacturer's instructions. It detects the hydroperoxides produced in the lipoxygenation reaction using a purified LOX and is used to screen for LOX enzyme inhibitors compared to standard (Quercetin) and expressed as μM . **In-vitro TAC assay:** This assay was investigated using Total Antioxidant Capacity (TAC) ELISA kit following the manufacturer's instructions compared to standard (ascorbic acid) and expressed as U/ml.

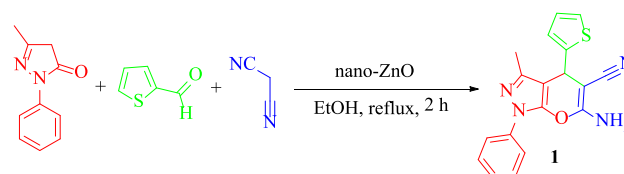
2.5. Statistical analysis

The results were expressed as the mean \pm S.D. and statistical comparisons were carried out using one-way analysis of variance (ANOVA) followed by Duncan's test. The minimal level of significance was identified at $P < 0.05$.

3. Result and discussion

3.1. Chemistry

One-pot multicomponent cyclocondensation conventions developed for the synthesis of 6-amino-3-methyl-1-phenyl-4-(thiophen-2-yl)-1,4-dihydropyrano[2,3-*c*]pyrazole-5-carbonitrile (**1**). This protocol is carried out by the reaction of 5-methyl-2-phenyl-2,4-dihydro-3H-pyrazol-3-one, thiophene-2-carbaldehyde malononitrile in the presence of a catalytic amount of supported metal nanoparticle ZnO as a catalyst using refluxing conditions in ethanol. Different catalysts were used to



Scheme 1. Synthesis of 6-amino-3-methyl-1-phenyl-4-(thiophen-2-yl)-1,4-dihydropyrano[2,3-*c*]pyrazole-5-carbonitrile (**1**).

Table 1

Optimization of the Reaction Conditions.

Entry	Solvent	Catalyst (base)	Temperature (°C)	Time (h)	Yield (%)
1	EtOH	AcONa	reflux	6	30
2	EtOH	Et_3N	reflux	5	45
3	EtOH	Piperidine	reflux	5	41
4	EtOH	AcONH_4	reflux	6	54
5	EtOH	ZnO Nanoparticles	reflux	2	85

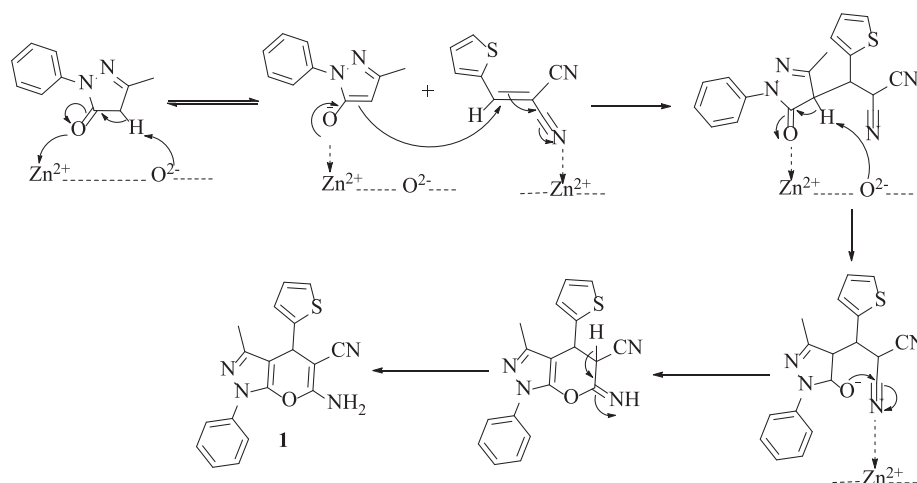
determine the optimum reaction conditions (Scheme 1).

To optimize the type of catalysts, AcONa, Et_3N , or piperidine, AcONH_4 and ZnO Nanoparticles were used in this experiment. The best results were obtained when ZnO Nanoparticles were used in the reaction. The results indicated low efficiency for AcONa. To optimize the time, the model reaction was carried out in ethanol at refluxing conditions. The results illustrate that 85% yield was obtained at 2 h (Table 1).

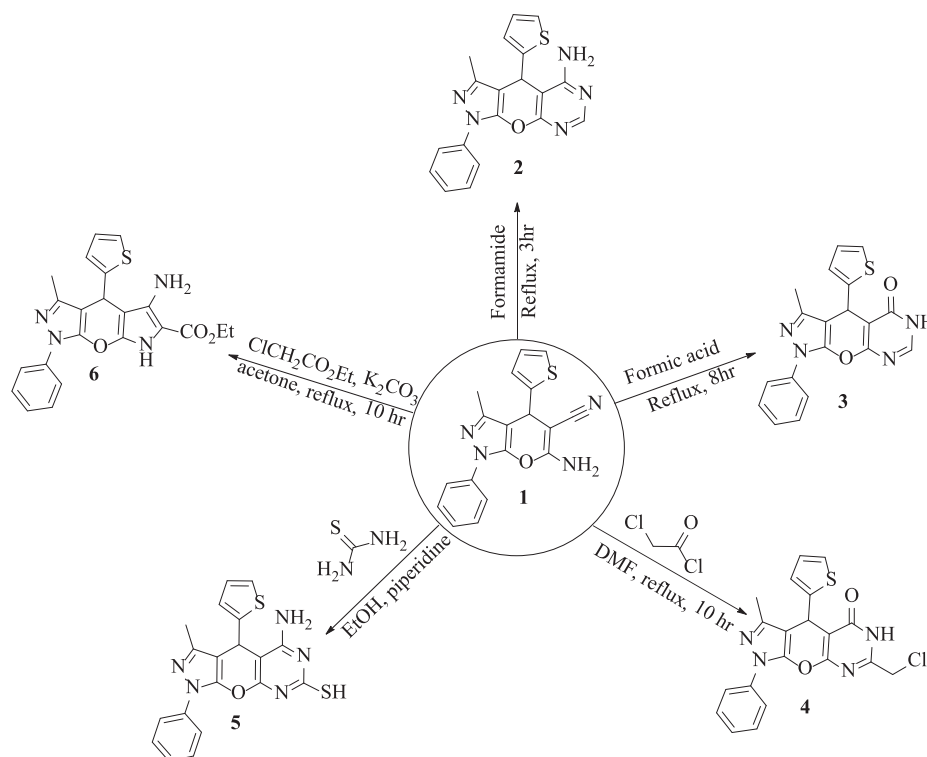
The structure of compound **1** was elucidated with IR, ^1H NMR, and ^{13}C NMR spectra, and elemental analysis data have been discussed for a representative compound **1**. The IR spectrum of **1** showed a sharp peak at 3456, 3312 cm^{-1} , which corresponds to the stretching frequency of the NH_2 group, and peaks at 2210 cm^{-1} correspond to the nitrile, respectively. The ^1H NMR spectra of **1** showed two singlets at δ 7.34 ppm for the $-\text{NH}_2$ protons (D_2O exchangeable), clearly indicating the incorporation of both moieties in the product. In contrast, the ^{13}C NMR spectrum showed a signal at (δ in ppm) 115.62 ppm due to the $\text{C}\equiv\text{N}$ group. A possible mechanism for the reaction is carried out according to the Knoevenagels-Michael reaction shown in (Scheme 2).

6-amino-3-methyl-1-phenyl-4-(thiophen-2-yl)-1,4-dihydropyrano[2,3-*c*]pyrazole-5-carbonitrile **1** was found to be an adequate key starting for the creation of some other new heterocyclic compounds, where it was heated in formamide for 3 h., to produce compound **2**. The spectral and analytical data of compound **2** confirmed its structure. The pyrimidinone derivative **3** was obtained on the one hand by refluxing compound **1** in excess formic acid. The IR spectrum substantiated the absorption bands pyrimidinone NH and $\text{C}=\text{O}$ respectively at their perspective values. ^1H NMR, MS, and elemental analysis gave the confirmatory data for compound **3** (cf. Scheme 3 and Experimental section). On the other hand, refluxing of compound **1** with chloroacetyl chloride in DMF resulted in the disappearance of the NH_2 signals in the IR and ^1H NMR spectra, respectively, due to the formation of 7-(chloromethyl)-3-methyl-1-phenyl-4-(thiophen-2-yl)-4,6-dihydropyrazolo[4',3':5,6]pyrano[2,3-*d*]pyrimidin-5(1H)-one **4**. While, Reactions of compound **1** with thiourea in boiling glacial acetic acid in the presence of a catalytic amount of HCl yielded 5-amino-3-methyl-1-phenyl-4-(thiophen-2-yl)-1,4-dihydropyrazolo[4',3':5,6]pyrano[2,3-*d*]pyrimidine-7-thiol **5**. The reaction of compound **1** with ethyl chloroacetate in the presence of a catalytic amount of anhydrous K_2CO_3 in dry acetone was stirred under reflux for 10 h provides Ethyl 5-amino-3-methyl-1-phenyl-4-(thiophen-2-yl)-4,7-dihydro-1H-pyrrolo[3',2':5,6]pyrano[2,3-*c*]pyrazole-6-carboxylate **6**, respectively (Scheme 3).

The cyclo condensation of compound **1** with *p*-nitrobenzaldehyde in the presence of a catalytic amount of piperidine yielded pyrazolopyr-anopyrimidone **7**. IR of **7** showed $\text{C}\equiv\text{N}$ disappearance, whereas its ^1H



Scheme 2. The plausible mechanism for the synthesis of 1,4-dihydropyranopyrazole-5-carbonitrile (1).

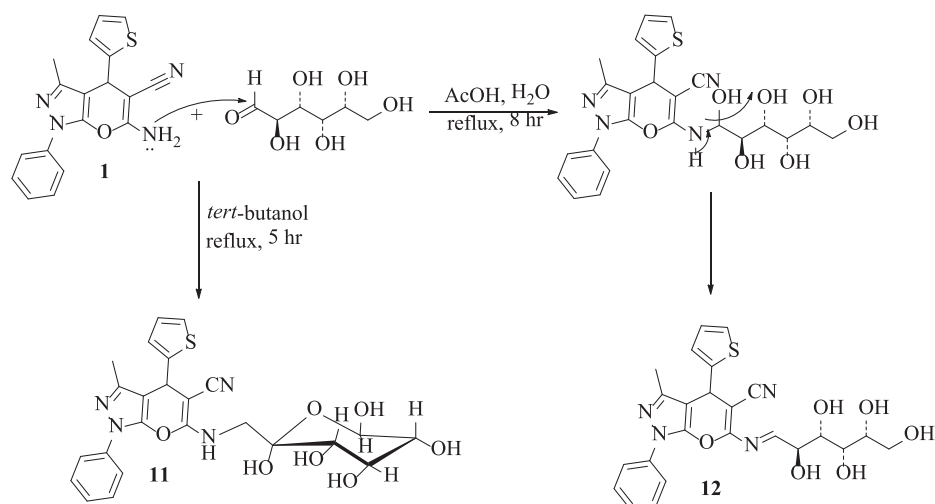
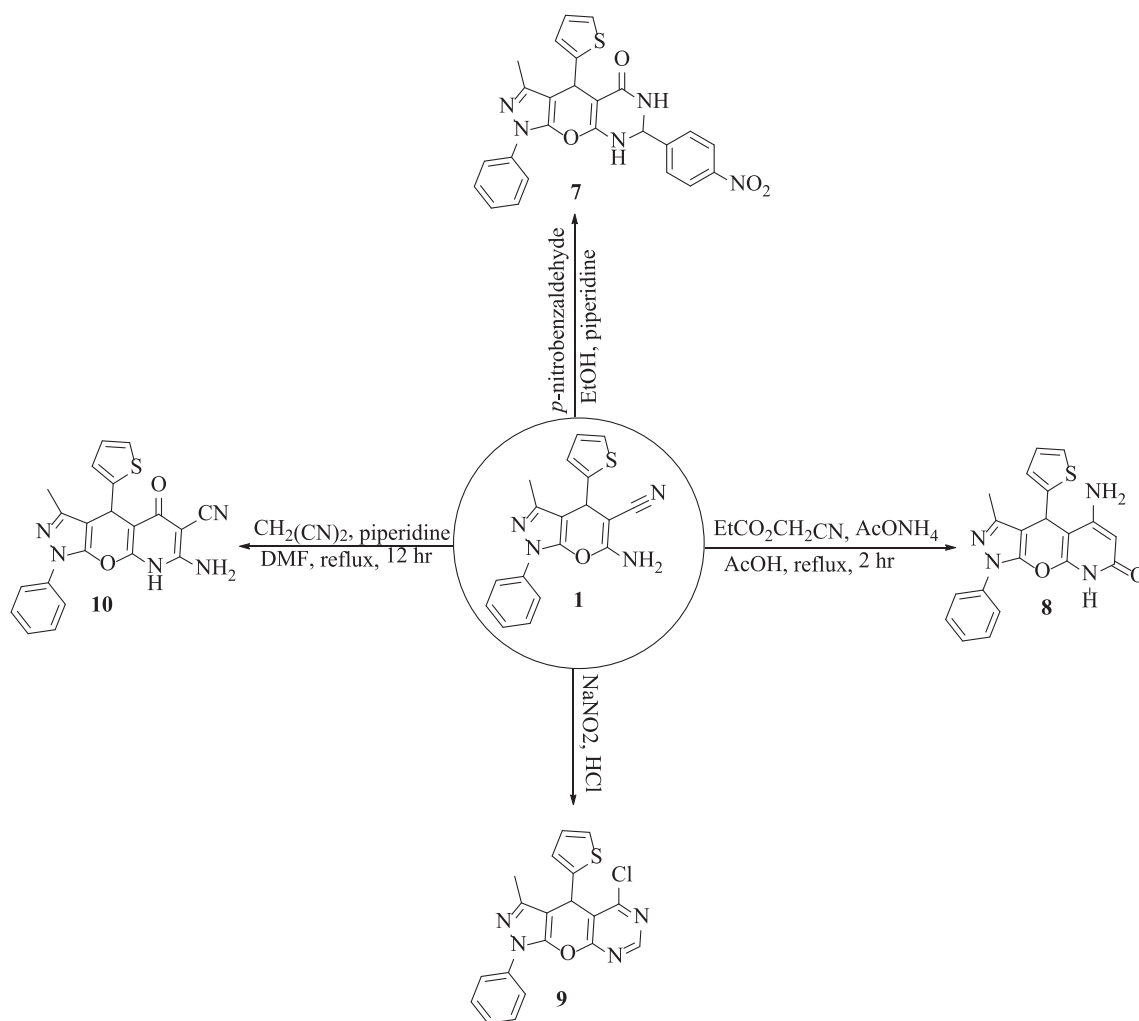


Scheme 3. Synthesis of highly functionalized Pyrano[2,3-c]Pyrazoles.

NMR showed two NH signals at $\delta = 9.87$ ppm. While, Reactions of compound **1** with ethyl cyanoacetate with ammonium acetate afforded 5-amino-3-methyl-1-phenyl-4-(thiophen-2-yl)-4,8-dihydropyrazolo [4',3':5,6]pyrano[2,3-b]pyridin-7(1H)-one **8**. Continuing a series of synthesis, the pyranopyrazole derivative **1** was transformed into 5-chloro-3-methyl-1-phenyl-4-(thiophen-2-yl)-1,4-dihydropyrazolo [4',3':5,6]pyrano[2,3-d]pyrimidine **9** by the addition of sodium nitrite solution to a suspended solution in concentrated hydrochloric acid at 0–5 °C with stirring at room temperature. While, the reaction of **1** with malononitrile in basic medium yielded the corresponding 7-amino-3-methyl-5-oxo-1-phenyl-4-(thiophen-2-yl)-1,4,5,8-tetrahydropyrazolo [4',3':5,6]pyrano[2,3-b]pyridine-6-carbonitrile **10**. The structure of compounds **9** and **10** were approved by IR, ^1H NMR, and elemental analysis (cf. [Scheme 4](#) and Experimental section).

The reaction of glucose with compound **1** amused depending on the

solvent used in the reaction, when the reaction performed in *tert*-butanol followed Maillard reaction pathway giving 3-methyl-6-(((2R,3S,4S,5R,6R)-2,3,4,5,6-pentahydroxytetrahydro-2H-pyran-yl)methyl)amino)-1-phenyl-4-(thiophen-2-yl)-1,4-dihydropyranopyrazolo[2,3-c]pyrazole-5-carbonitrile **11**. whilst, when the reaction carried out in acetic acid the main product is the Schiff base 3-methyl-6-(((2S,3S,4S,5R,E)-2,3,4,5,6-pentahydroxyhexylidene)amino)-1-phenyl-4-(thiophen-2-yl)-1,4-dihydropyranopyrazolo[2,3-c]pyrazole-5-carbonitrile **12**. The ^1H NMR spectra differentiate between the two compounds, the Schiff base compound **12** showed an olefinic proton absorption at $\delta = 7.43$ ppm; whereby compound **11** showed two signals $\delta = 3.35$ and 7.74 ppm due to CH_2 and NH groups ([Scheme 5](#)).



3.2. Structural parameters and models

3.2.1. 6-amino-3-methyl-1-phenyl-4-(thiophen-2-yl)-1,4-dihydropyrano [2,3-c]pyrazole-5-carbonitrile (1)

The molecule is slightly sterically-hindered, there are four aromatic

rings attached together, two aromatic rings as fused system 1,4-dihydropyrano[2,3-c]pyrazole and two separated rings, thiophen ring attached with fused aromatic system through the C1 of 1,4-dihydropyrano ring and phenyl ring through the N9 of pyrazole ring. The molecule is non planer, there is two plans, one plane occupied by the two

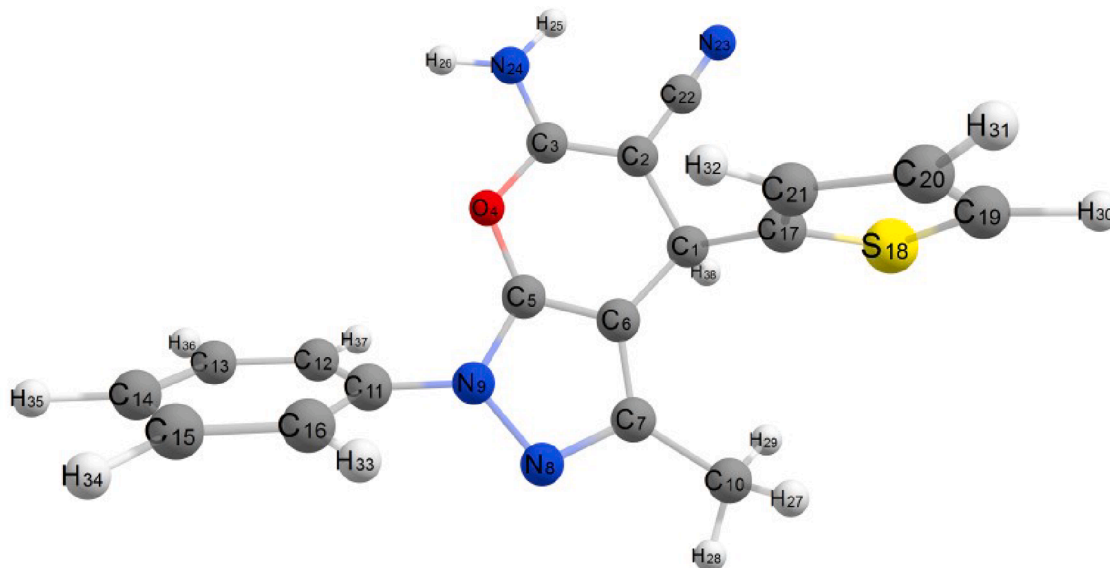


Fig. 2. Optimized geometrical structure of compound (1), 6-amino-3-methyl-1-phenyl-4-(thiophen-2-yl)-1,4-dihydropyrano[2,3-c]pyrazole-5-carbonitrile by using DFT calculations.

Table 2

Equilibrium geometric parameters bond lengths (Å), bond angles (°), dihedral angles (°), total energy (k cal/mol), heat of formation (k cal/mol) and dipole moment of the compound (1) by using DFT calculations.

Bond length (Å)			
C1—C2	1.535	C14—C15	1.342
C2—C3	1.366	C15—C16	1.343
C3—O4	1.369	C11—C16	1.343
O4—C5	1.361	C1—C17	1.523
C5—C6	1.369	C17—S18	1.473
C1—C6	1.531	S18—C19	1.456
C6—C7	1.419	C19—C20	1.338
C7—N8	1.353	C20—C21	1.336
N8—N9	1.362	C17—C21	1.340
C5—N9	1.343	C2—C22	1.417
N9—C11	1.345	C22—N23	1.163
C11—C12	1.343	C3—N24	1.364
C12—C13	1.342	C7—C10	1.497
C13—C14	1.342		
Bond angle (°)			
C1C17C21	124.63	O4C5N9	128.18
C1C17S18	28.02	C5N9C11	122.42
C2C1C17	109.64	C11N9N8	127.35
C17C1C6	109.79	N9C11C12	119.97
C2C22N23	179.19	N9C11C16	119.88
C1C2C22	119.31	C6C7C10	128.23
C3C2C22	119.13	N8C7C10	123.69
C2C3N24	119.24	C1C6C7	129.51
O4C3N24	117.18		
Dihedral angles (°)			
C21C17C1C2	63.06	N24C3O4C5	178.68
C21C17C1C6	-58.41	C10C7C6C5	179.89
S18C17C1C6	122.45	C12C11N9C5	67.68
S18C17C1C2	-116.08	C12C11N9N8	-121.34
N9C5O4C3	-178.90	C16C11N9N8	59.31
C1C6C7N8	-179.89	C16C11N9C5	-111.66
Total energy/ k cal/mol			-196.669
Heat of formation k cal/mol			-8696.662
Total dipole moment/D			3.775

aromatic rings of the fused aromatic system, 1,4-dihydropyrano[2,3-c]pyrazole and other plane occupied by the two separated aromatic rings, thiophen and phenyl. The two planes are perpendicular respect to others, the dihedral angles C21C17C1C2 and C21C17C1C6 are 63.06°

and -58.41°, respectively, while dihedral angles S18C17C1C6 and S18C17C1C2 are 122.45° and -116.08°, respectively. These values of dihedral angles confirmed that the thiophen ring is lying out of the plane occupied by 1,4-dihydropyrano[2,3-c]pyrazole. The dihedral angles C16C11N9N8 and C16C11N9C5 are 59.31° and -111.66°, respectively, while dihedral angles C12C11N9C5 and C12C11N9C8 are 67.68° and -121.39°, respectively. These values of dihedral angles confirmed that the phenyl group is lying out of the plane occupied by 1,4-dihydropyrano[2,3-c]pyrazole and the two rings, thiophen and phenyl are lying in the same plane as seen in Fig. 2. The C≡N group attached directly through C2, the bond angle C2C22N23 is 179.19° ≈ 180°, also all bond angles in this compound are varied from 109.64° to 129.51°, these values reflect that the type of sp² hybridization spreading over most atoms of the molecule except the carbon atom of cyano group -C≡N group, the angles C2C22N23, this value reflects that the type of hybridization on central carbon atom C22 of cyano group is sp [41], all bond angles and dihedral angles are listed in Table 2. The non planarity of the molecule play important rule in its activity and also in the biological activity, phenyl ring can be rotated around the nitrogen atom, N9 of pyrazole ring of the fused aromatic system out of the plane, also the thiophen ring can be rotated around the carbon atom, C1 of 1,4-dihydropyran ring out of the plane occupied by molecule. The value of energy of this compound is -196.669 k cal/mol and the heat of formation of this compound is -8696.662 k cal/mol. The presence of strong withdrawing groups as -C≡N group besides to other strong donating groups as -NH₂ and -CH₃ groups cause generation of weak dipole moment 3.775D. The all bonds in the phenyl group from C11 till C16 with bond lengths varied between 1.342 and 1.343 Å [42] are the shortest C—C bonds in whole molecule. The C7—N8 and C5—N9 bond lengths are 1.353 and 1.343 Å [43] are significantly shorter than N8—N9 bond length 1.362 Å [42], there is a single bond characters N9 and C5 atoms [44], the bond lengths of C2—C3 and C5—C6 are 1.366 and 1.369 Å, whereas these bonds have double bond characters [45], while the bond lengths of C1—C2, C1—C6 are 1.535 and 1.531 Å, also the bond lengths of C3—O4 and C5—O4 are 1.369 and 1.361 Å these values reflected that presence of a single bond characters. The bond lengths between atoms are listed in the Table 2, these values are compared nicely with crystal structure of the molecule has the similar structure [43]. The S18—C19 bond length is 1.456 Å [46], this bond is shorter than C17—S18 bond length is 1.473 Å [46], these values reflects that there is a single bond characters between the S18 atom and others bonded carbon atoms with it. Detailed analysis of

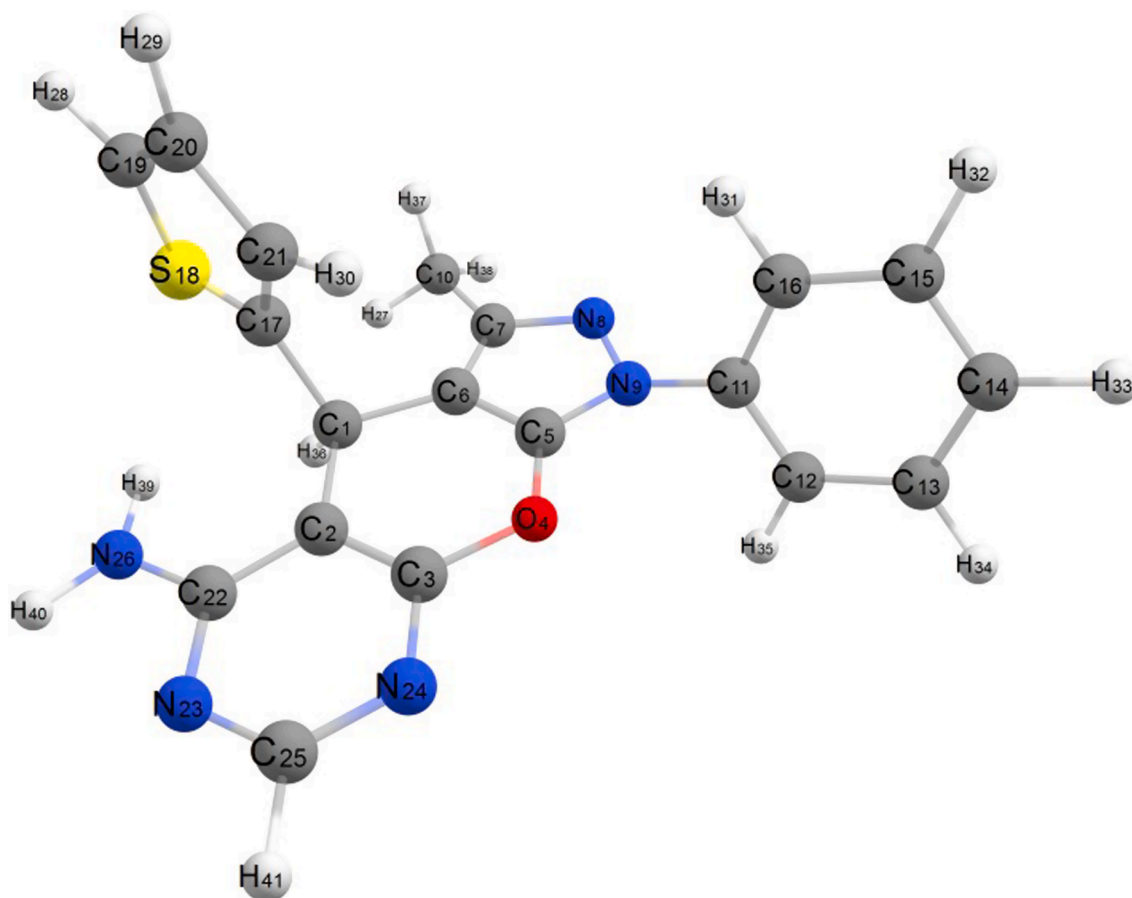


Fig. 3. Optimized geometrical structure of compound (2), 3-methyl-1-phenyl-4-(thiophen-2-yl)-1,4-dihydropyrazolo[4',3':5,6]pyrano[2,3-d]pyrimidin-5-amine by using DFT calculations.

corresponding bond lengths in various hetero cyclic compounds were given elsewhere [43,47]. All distances and angles between the atoms of the ligand are given in Table 2.

3.2.2. 3-methyl-1-phenyl-4-(thiophen-2-yl)-1,4-dihydropyrazolo[4',3':5,6]pyrano[2,3-d]pyrimidin-5-amine (2)

Fig. 3 showed the optimized geometrical structures of the compounds (2). The molecule is non planer, there is two plans, one of them is occupied by dihydropyrazolo[4',3':5,6]pyrano[2,3-d]pyrimidin aromatic system and the other plane is occupied by thiophen and phenyl rings. All bond lengths of this compound is similar to the bond lengths of compound (1). The dihedral angles of this compound as C16C11N9N8 and C16C11N9C5 are 57.75° and -99.01°, respectively, also the dihedral angles C12C11N9N8 and C12C11N9C5 are -124.63° and 78.59°, respectively, these values confirmed that phenyl group is lying out of the plane occupied the fused aromatic rings. The dihedral angles S18C17C1C2 and S18C17C1C6 are -123.76° and 116.06°, respectively, these values confirmed that the thiophen ring is lying out of the plane occupied by fused aromatic rings. The value of bond angles around the carbon atoms in this compound are varied between (116.47 and 128.40). Also the angles around the nitrogen atoms in the compound are varied between (117.53° and 132.74°), these values reflect that the type of sp^2 hybridization spreading over most atoms of the this compound. The energy of the compound (2) has lower value -213.859 k cal/mol less than that of the energy of compound (1), the heat of formation of compound (2) is -8900.158 k cal/mol. The dipole moment of compound (2) is 2.095D, this value is lower than the dipole moment of compound (1), it attributed to the absence of $-C\equiv N$ group in compound (2). The C2—C3 bond with bond length of 1.381 [48] Å is the longest C—C bond in whole molecule [49]. The C3—N24 and C2—C22

bond lengths are 1.349 and 1.376 Å, respectively [49], whereas these bonds have double bond characters [45] also the N23—C22 and C25—N23 bond lengths are 1.340 and 1.355 Å [49], there is a single bond characters N and C atoms [44]. The length of the N—C bonds (1.340–1.355 Å) in the dihydropyrazolo[4',3':5,6]pyrano[2,3-d]pyrimidine aromatic system indicate the conjugation between the lone pair of the nitrogen atoms and p-system of the pyrimidin group [50].

3.2.3. 3-methyl-1-phenyl-4-(thiophen-2-yl)-4,6-dihydropyrazolo[4',3':5,6]pyrano[2,3-d]pyrimidin-5(1H)-one (3)

Fig. 4 showed the optimized geometrical structures of the compound (3), this compound is similar to compound (2) in all parameters and structure with replacement of $-NH_2$ group attached with pyrimidin ring with $C=O$ group in the same atom. The energy of the compound (3) has lower value -219.457 k cal/mol less than that of the energy of compound (1) and higher than the energy of compound (2), the heat of formation of compound (3) is -8760.918 k cal/mol, the presence of $C=O$ group attached to pyrimidin ring instead of NH_2 group causing rising of the value of dipole moment, 5.593D more than compound (2).

3.2.4. 7-(chloromethyl)-3-methyl-1-phenyl-4-(thiophen-2-yl)-4,6-dihydropyrazolo[4',3':5,6]pyrano[2,3-d]pyrimidin-5(1H)-one (4)

The optimized geometrical structures of the compounds (4) is shown in Fig. 5, this compound has the same structure features of the compound (3) with adding of $ClCH_2-$ group to the pyrimidine ring in the carbon atom C25, lying between the two nitrogen atoms N23 and N24 of pyrimidine ring. The presence of $ClCH_2-$ group causes lowering of the total energy value by 22.056 k cal/mol. The energy of this compound, -241.974 k cal/mol is less than the energy of compound (3), also the heat of formation of compound (4) is -9309.978 k cal/mol. The

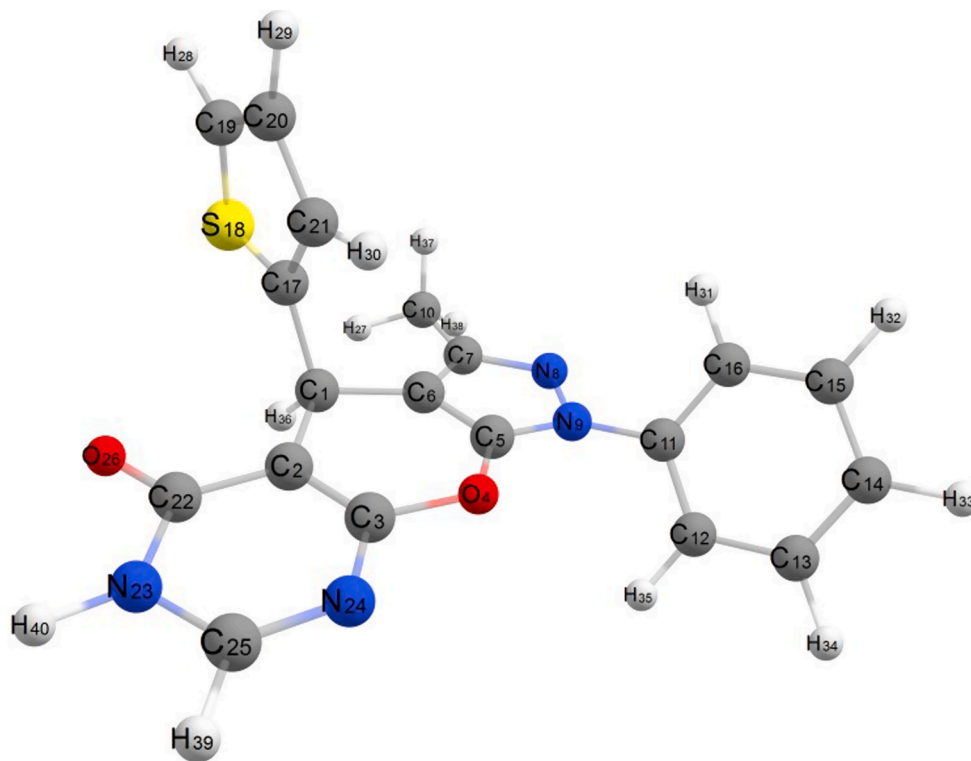


Fig. 4. Optimized geometrical structure of compound (3), 3-methyl-1-phenyl-4-(thiophen-2-yl)-4,6-dihydropyrazolo[4',3':5,6]pyrano[2,3-d]pyrimidin-5(1H)-one by using DFT calculations.

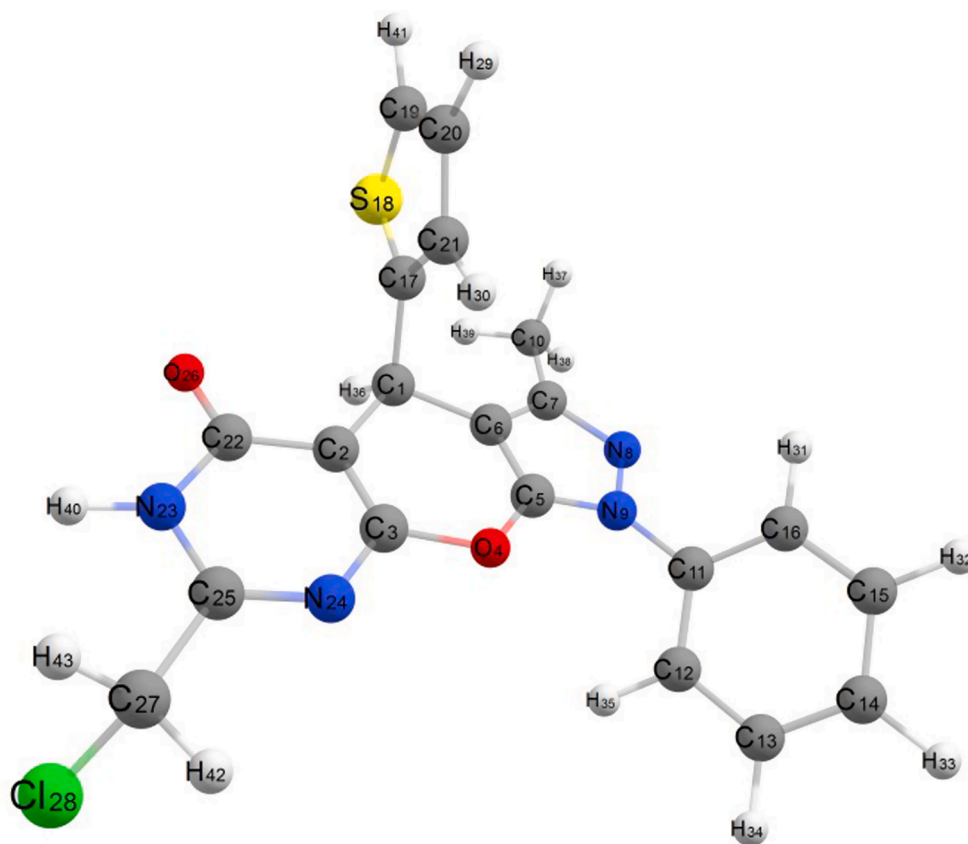


Fig. 5. Optimized geometrical structure of compound (4), 7-(chloromethyl)-3-methyl-1-phenyl-4-(thiophen-2-yl)-4,6-dihydropyrazolo[4',3':5,6]pyrano[2,3-d]pyrimidin-5(1H)-one by using DFT calculations.

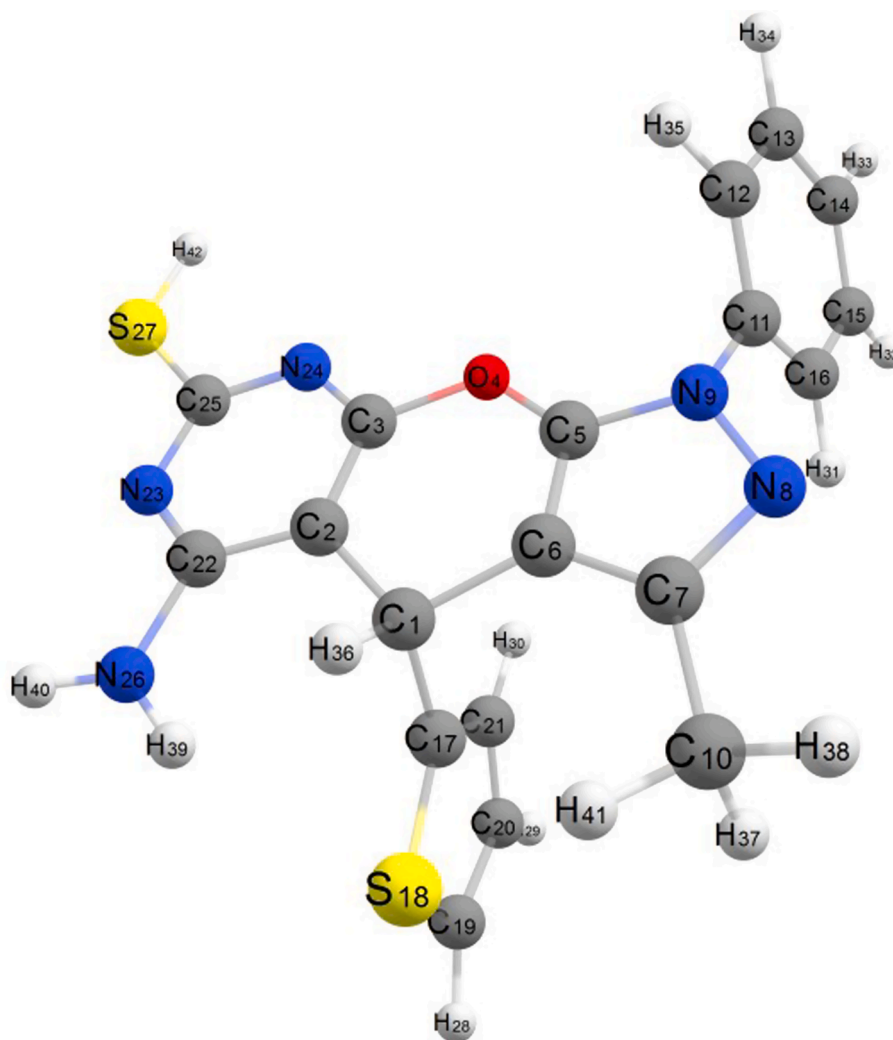


Fig. 6. Optimized geometrical structure of compound (5), 5-amino-3-methyl-1-phenyl-4-(thiophen-2-yl)-1,4-dihydropyrazolo[4',3':5,6]pyrano[2,3-d]pyrimidine-7-thiol by using DFT calculations.

presence of C=O and Cl groups attached to pyrimidin ring causing rising of the value of dipole moment, 5.879D more than compound (3).

3.2.5. 5-amino-3-methyl-1-phenyl-4-(thiophen-2-yl)-1,4-dihydropyrazolo[4',3':5,6]pyrano[2,3-d]pyrimidine-7-thiol (5)

The optimized geometrical structures of the compounds (5) is shown in Fig. 6, this compound has the same structure features of the compound (3) with presence of -SH group to the pyrimidine ring in the carbon atom C25, instead of ClCH₂-on the pyrimidine ring. The presence of -SH group causes lowering of the total energy value by 5.174 k cal/mol, but not less than compound (4). The energy of this compound, -224.631 k cal/mol is less than the energy of compound (3), also the heat of formation of compound (5) is -8997.226 k cal/mol. The presence of C=O and -SH groups attached to pyrimidin ring causing lowering of the value of dipole moment, 2.798D more than compound (3).

3.2.6. Ethyl-5-amino-3-methyl-1-phenyl-4-(thiophen-2-yl)-4,7-dihydro-1H pyrrolo[3',2':5,6]pyrano[2,3-c]pyrazole-6-carboxylate (6)

Fig. 7 showed the optimized geometrical structures of the compound (6), this compound is similar to compound (5) in all parameters and structure with replacement of pyrimidine ring attached with -NH₂ with pyrrol group. The energy of the compound (6) has lower value -268.019 k cal/mol less than that of the energy of compound (5), the heat of

formation of compound (6) is -921851.487 k cal/mol, the presence of R-COO- group attached to pyrrol ring with -NH₂ group causing slightly increasing of the value of dipole moment, 2.935D more than compound (5).

3.2.7. 3-methyl-7-(4-nitrophenyl)-1-phenyl-4-(thiophen-2-yl)-4,6,7,8-tetrahydro pyrazolo[4',3':5,6]pyrano[2,3-d]pyrimidin-5(1H)-one (7)

Fig. 8 showed the optimized geometrical structures of the compound (7), this compound is similar to compounds (3) and (4) in all parameters and structure with presence of nitrophenyl group attached with pyrimidine ring in C25. The energy of the compound (7) has lower value -309.987 k cal/mol less than that of the energy of compounds (3) and (4), the heat of formation of compound (7) is -11721.494 k cal/mol, the presence of nitrophenyl group attached to pyrimidin ring causing increasing of the value of dipole moment, 6.976D more than compounds (3) and (4).

3.2.8. 5-amino-3-methyl-1-phenyl-4-(thiophen-2-yl)-4,8-dihydropyrazolo[4',3':5,6]pyrano[2,3-b]pyridin-7(1H)-one (8)

The optimized geometrical structures of the compounds (8) is shown in Fig. 9, this compound has the same structure features of the compounds (2) and (5) with presence of C=O group to the pyridine ring in the carbon atom C25. The presence of C=O group causes lowering of the total energy value less than compounds (2) and (5). The energy of this

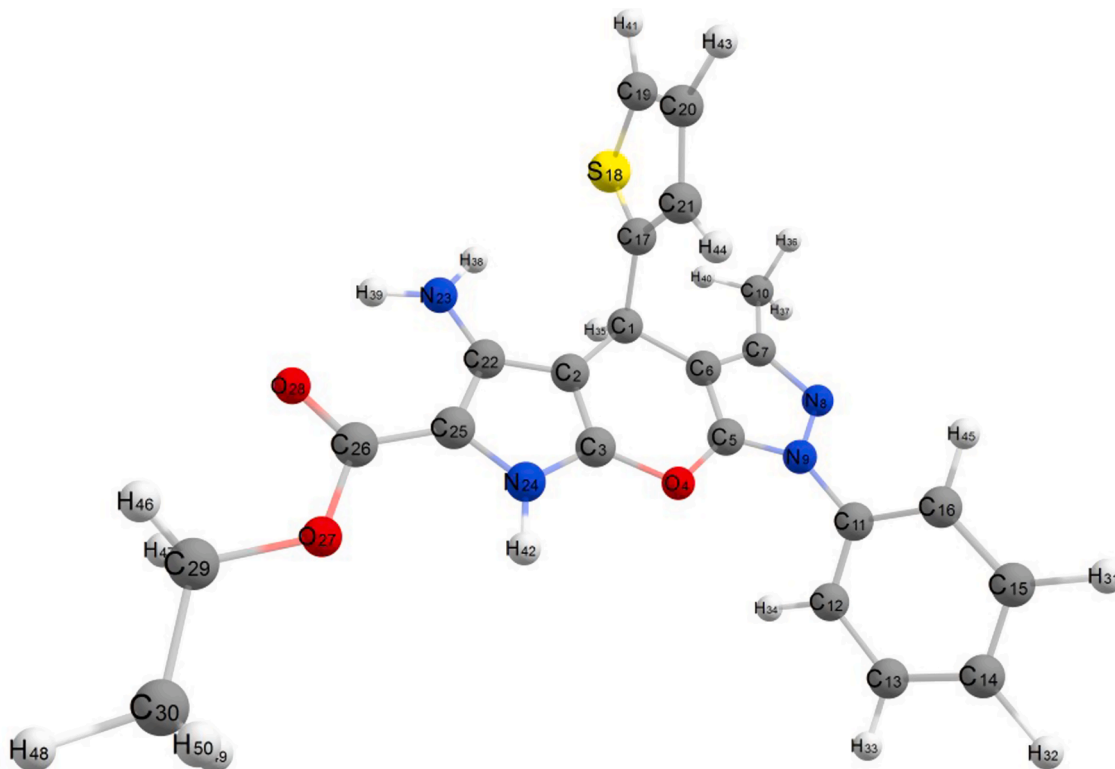


Fig. 7. Optimized geometrical structure of compound (6), Ethyl 5-amino-3-methyl-1-phenyl-4-(thiophen-2-yl)-4,7-dihydro-1H-pyrrolo[3',2':5,6]pyrano[2,3-c]pyrazole-6-carboxylate by using DFT calculations.

compound, -230.985 k cal/mol, also the heat of formation of compound (8) is -9071.547 k cal/mol. The presence of C=O groups attached to pyridine ring causing rising of the value of dipole moment, 5.697D more than compounds (2) and (5).

3.2.9. 5-chloro-3-methyl-1-phenyl-4-(thiophen-2-yl)-1,4-dihydropyrazolo[4',3':5,6]pyrano[2,3-d]pyrimidine (9)

Fig. 10 showed the optimized geometrical structures of the compound (9), this compound is similar to compound (2) in all parameters and structure with replacement of -NH_2 group attached with pyrimidin ring with -Cl group in the same atom. The energy of the compound (9) has lower value -216.878 k cal/mol less than that of the energy of compound (2), the heat of formation of compound (3) is -8637.846 k cal/mol, the presence of -Cl group attached to pyrimidin ring instead of NH_2 group causing slightly rising of the value of dipole moment, 2.998D more slightly higher than compound (2).

3.2.10. 7-amino-3-methyl-5-oxo-1-phenyl-4-(thiophen-2-yl)-1,4,5,8-tetrahydro pyrazolo[4',3':5,6]pyrano[2,3-b]pyridine-6-carbonitrile (10)

The optimized geometrical structures of the compounds (10) is shown in Fig. 11, this compound has the same structure features of the compound (8) with presence of $\text{C}\equiv\text{N}$ group to the pyridine ring in the carbon atom C23. The presence of $\text{C}\equiv\text{N}$ group causes lowering of the total energy value less than compound (8) by 12.711 k cal/mol. The energy of this compound, -243.696 k cal/mol, also the heat of formation of compound (10) is -9627.488 k cal/mol. The presence of $\text{C}\equiv\text{N}$ group attached to pyridine ring causing rising of the value of dipole moment, 12.592D more than compound (8).

3.2.11. 3-methyl-6-(((2R,3S,4S,5R,6R)-2,3,4,5,6-pentahydroxytetrahydro-2H-pyran-2-yl)methyl)amino)-1-phenyl-4-(thiophen-2-yl)-1,4-dihydropyrano [2,3-c]pyrazole-5-carbonitrile (11)

Fig. 12 showed the optimized geometrical structures of the compounds (11). The molecule is non planer. The value of bond angles

around the carbon atoms in this compound are varied between (111.78 and 129.51). Also the angles around the nitrogen atoms in two compounds are varied between (117.53° and 132.74°), these values reflect that the type of sp^2 hybridization spreading over most atoms of the this compound. The energy of the compound (11) has lower value -343.876 k cal/mol less than that of the energy of compound (1), the heat of formation of compound (11) is -12081.936 k cal/mol. The dipole moment of compound (11) is 5.894D, this value is higher than the dipole moment of compound (1), it attributed to the absence of $\text{-C}\equiv\text{N}$ group with presence of 2,3,4,5,6-pentahydroxytetrahydro-2H-pyran-2-yl ring attached with -NH group through -CH_2 in compound (11). The bond lengths of the N-C bonds varied between (1.346 – 1.354 Å) in the dihydropyrazolo[4',3':5,6]pyrano[2,3-d]pyrimidin aromatic system indicate the conjugation between the lone pair of the nitrogen atoms and p-system of the pyrimidin group [50].

3.2.12. 3-methyl-6-(((2S,3S,4S,5R,E)-2,3,4,5,6-pentahydroxyhexylidene)amino)-1-phenyl-4-(thiophen-2-yl)-1,4-dihydropyrano[2,3-c]pyrazole-5-carbonitrile (12)

Fig. 13 showed the optimized geometrical structures of the compound (12), this compound is similar largely to compound (11) in all parameters and structure with replacement of 2,3,4,5,6-pentahydroxytetrahydro-2H-pyran-2-yl ring with group attached with 2,3,4,5,6-pentahydroxyhexylidene group in the same atom. The energy of the compound (12) has lower value -351.793 k cal/mol less than that of the energy of compound (11) by 7.917 k cal/mol, the heat of formation of compound (12) is -12430.749 k cal/mol, the presence of 2,3,4,5,6-pentahydroxytetrahydro-2H-pyran-2-yl group as open chain attached to pyran ring instead of 2,3,4,5,6-pentahydroxytetrahydro-2H-pyran-2-yl group causing rising of the value of dipole moment with greater value 9.498D more higher than compound (11).

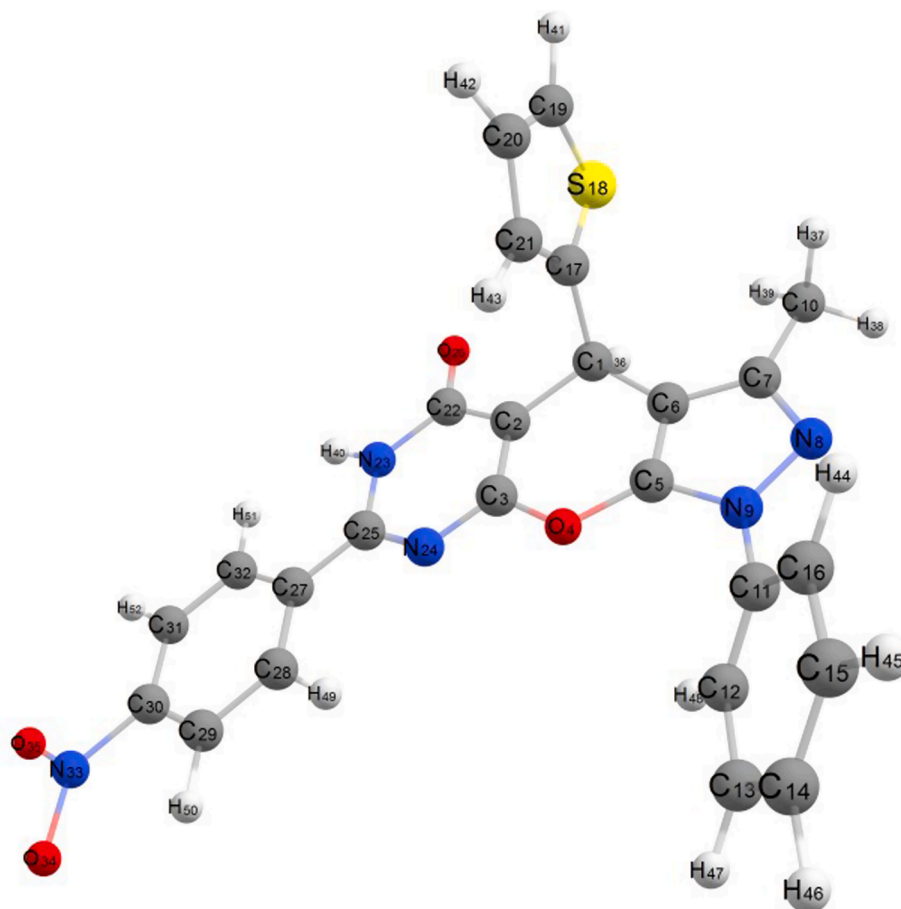


Fig. 8. Optimized geometrical structure of compound (7), 3-methyl-7-(4-nitrophenyl)-1-phenyl-4-(thiophen-2-yl)-4,6,7,8-tetrahydropyrazolo[4',3':5,6]pyrano[2,3-d]pyrimidin-5(1H)-one by using DFT calculations.

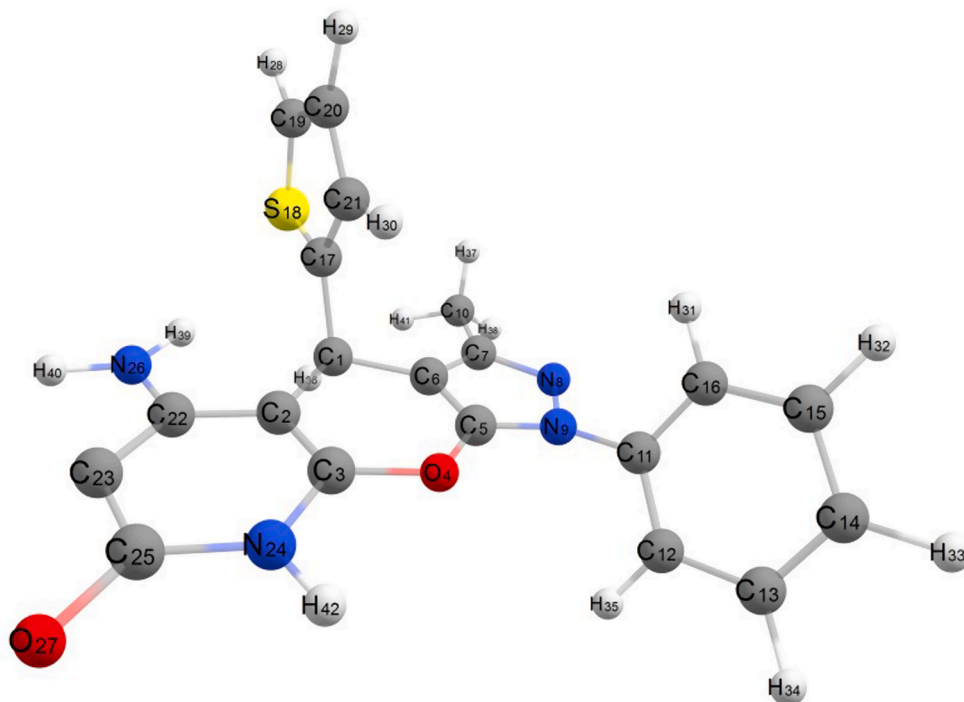


Fig. 9. Optimized geometrical structure of compound (8), 5-amino-3-methyl-1-phenyl-4-(thiophen-2-yl)-4,8-dihydropyrazolo[4',3':5,6]pyrano[2,3-b]pyridin-7(1H)-one by using DFT calculations.

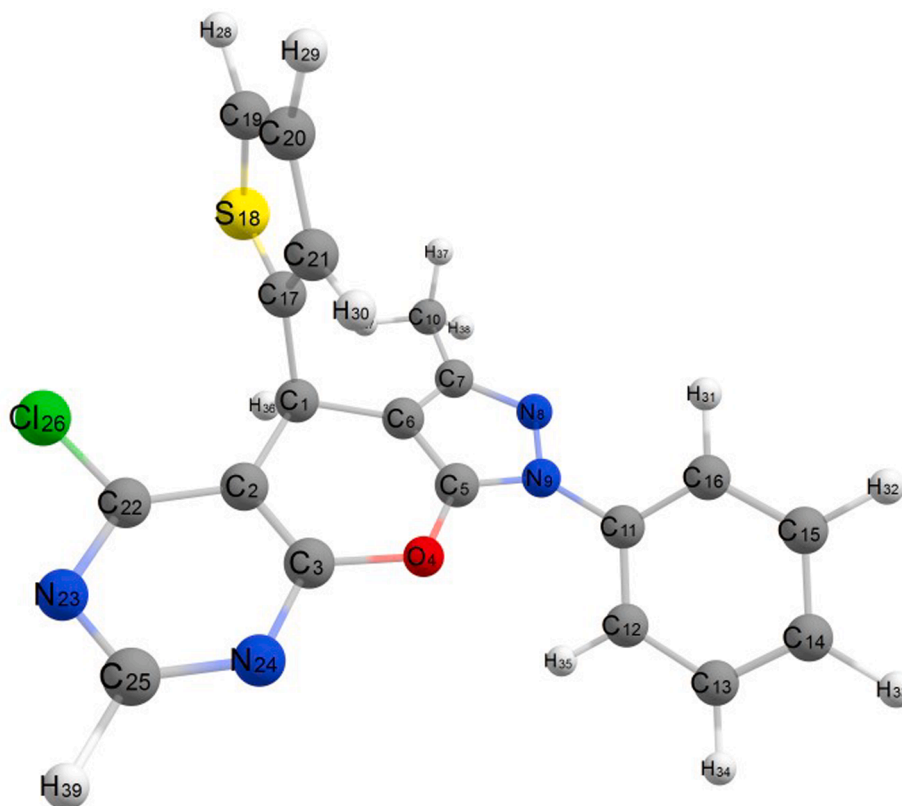


Fig. 10. Optimized geometrical structure of compound (9), 5-chloro-3-methyl-1-phenyl-4-(thiophen-2-yl)-1,4-dihydropyrazolo[4',3':5,6]pyrano[2,3-d]pyrimidine by using DFT calculations.

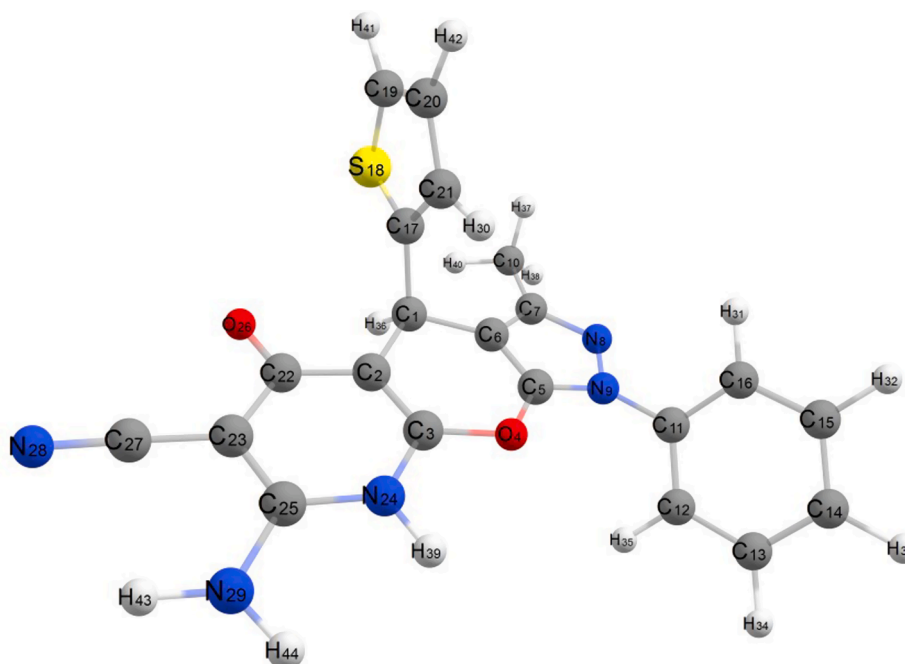


Fig. 11. Optimized geometrical structure of compound (10), 7-amino-3-methyl-5-oxo-1-phenyl-4-(thiophen-2-yl)-1,4,5,8-tetrahydropyrazolo[4',3':5,6]pyrano[2,3-b]pyridine-6-carbonitrile by using DFT calculations.

3.3. Charge distribution analysis

The charge distribution analysis on the optimized geometry configuration of the all studied compounds was made on the basis of natural

population analysis (NPA). The charge distribution on the hetero atoms, nitrogen, oxygen and sulfur of the different studied compounds indicates the presence of a net negative pole attributed to the presence of polar atoms beside the non planarity of these molecules, as a result the

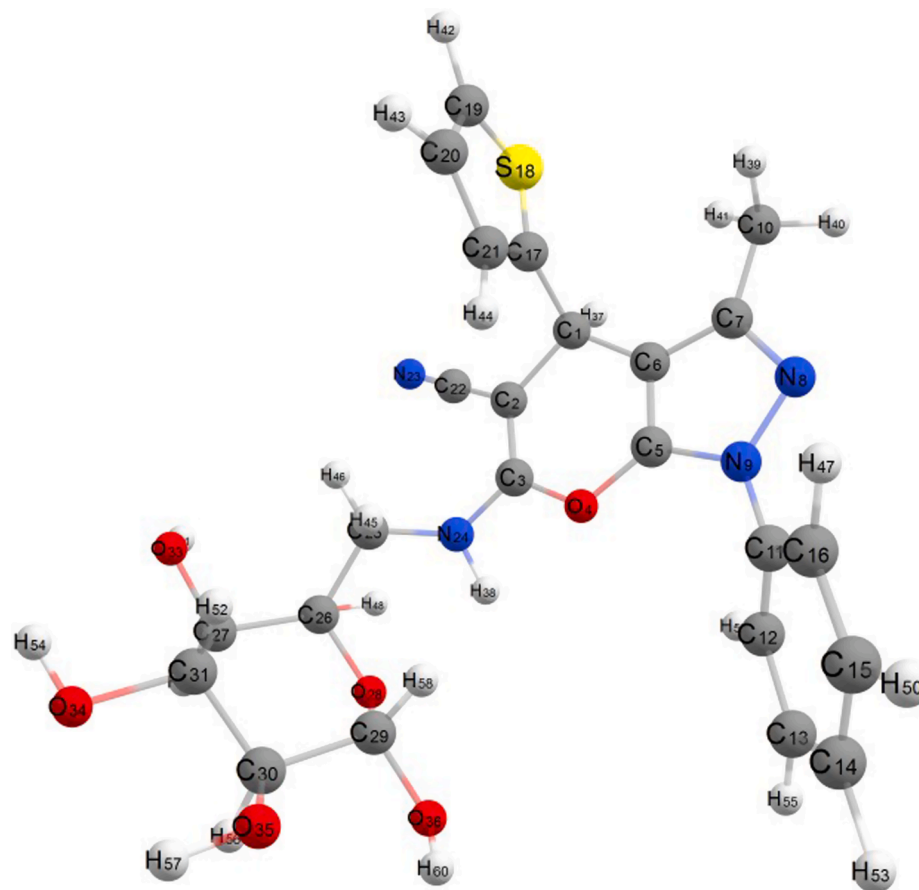


Fig. 12. Optimized geometrical structure of compound (11), 3-methyl-6-(((2R,3S,4S,5R,6R)-2,3,4,5,6-pentahydroxytetrahydro-2H-pyran-2-yl)methyl)amino)-1-phenyl-4-(thiophen-2-yl)-1,4-dihydropyran-2,3-c]pyrazole-5-carbonitrile by using DFT calculations.

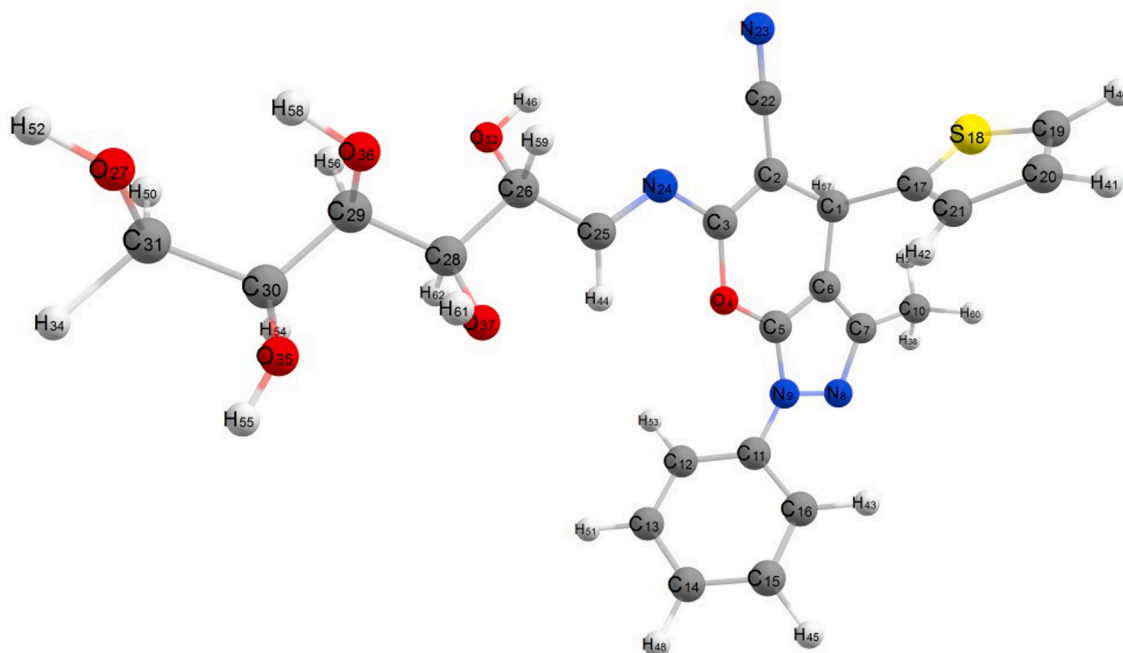


Fig. 13. Optimized geometrical structure of compound (12), 3-methyl-6-(((2S,3S,4S,5R,E)-2,3,4,5,6-pentahydroxyhexylidene)amino)-1-phenyl-4-(thiophen-2-yl)-1,4-dihydropyran-2,3-c]pyrazole-5-carbonitrile by using DFT calculations.

molecules are a slightly high dipole for the $\text{—C}\equiv\text{N}$ compounds, while the —NH_2 compounds have slightly weak dipole. There is building up of charge density on the donating nitrogen, oxygen and sulfur atoms involved in the 1,4-dihydropyranopyrazole and thiophen ring in the compound (1), the highest charged atoms are N23 (-0.311) of $\text{—C}\equiv\text{N}$ group, N24 (-0.364) of terminal amino group and N8 (-0.259) of 1,4-dihydropyranopyrazole ring, the charge accumulated on N9 of 1,4-dihydropyranopyrazole ring is -0.002 , there is a small charge accumulated on sulfur atom S18 of thiophen ring is 0.034 and the most carbon atoms have possessed negative charge density except C1, C3, C5 and C7 of the 1,4-dihydropyranopyrazole. The variation on the charge accumulation on all atoms in compound (1) causes generating of a negative pole on the $\text{—C}\equiv\text{N}$ group.

Also, in case of compound (2), there is a definite atoms have possessed accumulation of charge on it more than other atoms. The charge accumulated on oxygen atom O4 and nitrogen atom N8 are (-0.289 and -0.263), while nitrogen atom N9 of 1,4-dihydropyranopyrazole ring has lower negative charge (-0.009). The charge accumulated on the two nitrogen atoms of pyrimidin ring N23 and N24 are (-0.339 and -0.326) and nitrogen atom N26 of amino group —NH_2 attached with pyrimidin ring is -0.385 , the more positive charges are located on C3, C5, C22 and C37 (0.398 , 0.289 , 0.369 and 0.289 , respectively).

In compound (3), there is building up of charge density on the oxygen atom O26, -0.479 and carbon atom C22, 0.443 of pyrimidin-5(1H)-one ring. Also, there is building up of charge density on the two nitrogen atoms N23 and N24 of pyrimidin-5(1H)-one ring, -0.234 and -0.303 , while the charge density on the two nitrogen atoms N8 and N9 of 4,6-dihydropyrazolo are -0.262 and -0.005 . the more positive charges accumulated on carbon atoms are localized on C3, C22 and C37 as shown 0.399 , 0.442 and 0.272 , respectively. These values of charge densities over atoms producing slightly large dipole 5.593 .

In compound (4), These values of charges over all atoms produced a slightly large dipole moment, 5.879D . The charge density on O4, N8 and N9 of the 4,6-dihydropyrazolo[4',3':5,6]pyran ring are -0.286 , -0.261 and -0.004 , respectively. Also the charge density on the hetero atoms of the pyrimidin-5(1H)-one ring N23, N24 and O26 are -0.245 , -0.317 and -0.466 , respectively, while the positive charges are localized over carbon atoms, C3, C5, C22 and C37 as, 0.398 , 0.248 , 0.446 and 0.322 , respectively. Also there is a significant negative charge accumulated on the Cl28, -0.247 , so there is negative pole spreading over all hetero atoms and positive pole over carbon atoms, these poles causing slightly large dipole moment.

In the compound (5), the presence of —SH group decreases the value of dipole moment, 2.798D . the negative charge densities are localized on the O4 and N8 of the 1,4-dihydropyrazolo[4',3':5,6]pyran, -0.286 and -0.261 , nitrogen atoms N23 and N24 of sulfur atom S27 of [2,3-d]pyrimidine-7-thiol ring, (-0.355 , -0.359 and -0.428) respectively and nitrogen atom, N26 of amino group attached with [2,3-d]pyrimidine-7-thiol ring, -0.382 . The positive charge densities are spreading over most carbon atoms, as C3, C5, C22 and C25, 0.411 , 0.252 , 0.383 and 0.482 , respectively. There is no large difference between the two charged poles, so there is a weak dipole.

In case of compound (6), there is a small difference between the negative charge density and positive charge density, this small value causing lowering of dipole value. The negative charge densities are localized on N8 of the pyrazole ring, -0.265 , N24 of the 4,7-dihydro-1H-pyrrole ring, -0.363 and the two oxygen atoms of the carboxylate group —COO— , O27 and O28, -0.329 and -0.461 , while the positive charge densities are spreading over most carbon atoms specially C26 of carboxylate group, 0.498 .

The dipole moment value in the compound (7) is slightly high, 6.976D . There slightly large difference between negative and positive charge on atoms of this compound, the most negative charges are localized over hetero atoms, as O4, N8 of 4,8-dihydropyrazolo[4',3':5,6]pyran ring, -0.298 and -0.265 , two nitrogen atoms N23, N24 and

oxygen atom O26 of [2,3-d]pyrimidin-5(1H)-one ring, -0.274 ,

-0.355 and -0.479 , also the two oxygen atoms O34 and O35 of nitrophenyl group, -0.315 and -0.314 . The positive charge densities spreading over most carbon atoms, as C3, C5, C22 and C25, 0.403 , 0.248 , 0.445 and 0.348 , respectively and nitrogen atom N33 of nitrophenyl group, 0.235 . These values of charge densities play important rule in the generation of large dipole, specially the presence of nitrophenyl group in this compound.

Compound (8) has possessed slightly higher dipole moment, 5.697D . The presence of strong withdrawing group as C=O group in this compound as [2,3-b]pyridin-7(1H)-one causes formation of a negative pole, the charge density on the oxygen atom O27 is -0.449 , more negative charge, also there is more negative charge (-0.379) on the nitrogen atom N26 of amino group. The more positive charge densities are localized over most carbon atoms, as C3, C5, C22 and C25, 0.384 , 0.249 , 0.415 and 0.538 .

In compound (9), there is a weak dipole can be obtained from the presence of —Cl group attached with [2,3-d]pyrimidine, there is no significant building of charge densities on atoms, the negative charge densities on oxygen atom O4, -0.279 and nitrogen atom N8, -0.258 of 1,4-dihydropyrazolo[4',3':5,6]pyran ring, also the two nitrogen atoms N23 and N24 of the pyrimidine ring, -0.268 and -0.285 , there is a negative charge on the Cl26, -0.298 . The positive charge densities are spreading over most carbon atoms specially, C22 and C25, 0.399 and 0.278 . From these values of charge densities, there is no large difference between positive and negative charges can be created to produce large dipole value.

Compound (10) has possessed greater dipole moment value 12.592D , from the studying of the charge densities over all atoms of this compound it found that, the summation of negative charges over hetero atoms, specially oxygen atom O26, nitrogen atoms, N24, N28 and N29 of 7-amin-5-oxo-[2,3-b]pyridine-6-carbonitrile group are -0.458 , 0.218 , -0.345 and -0.359 , respectively. There is small positive charge densities over all atoms compared with negative charge densities, the more positive charged atoms are C3, C5, C22 and C25, 0.333 , 0.244 , 0.374 and 0.351 . these values reflects that there is a greater negative pole can be produced on this compound with formation small positive pole. in case of compound (11) and compound (12), they have the same structure but there is important difference, in compound (11), there is a cyclic saturated hydrocarbon as 2,3,4,5,6-pentahydroxytetrahydro-2H-pyran ring was used, while in compound (12), there is straight long chain of hydrocarbon was used as 2,3,4,5,6-pentahydroxyhexylidene. This difference in the substitution effects largely on the distribution of charge densities over all atoms of these compounds and also effects on the value of dipole moment. In compound (11), the dipole moment value 5.894D is lower than the value of dipole moment of compound (12), 9.498D . In compound (11), all oxygen atoms have possessed negative charge densities varied from -0.284 on oxygen atom O4 of 1,4-dihydropyran ring to -0.389 on the O36 of 2,3,4,5,6-pentahydroxytetrahydro-2H-pyran-2-yl ring, also nitrogen atoms have a negative charge densities varied from -0.021 on N9 of pyrazole ring to -0.286 on N23 of cyano group. The positive charge densities are localized on most carbon atoms specially atoms of 2,3,4,5,6-2,3,4,5,6-pentahydroxytetrahydro-2H-pyran-2-yl ring. In case of compound (12), there is a significant building up of a negative charge densities spreading over all hetero atoms specially oxygen atoms of 2,3,4,5,6-pentahydroxyhexylidene, these values of charge densities varied from -0.281 on O4 of 1,4-dihydropyran ring to -0.378 on the O27 of 2,3,4,5,6-pentahydroxyhexylidene group. The positive charge densities are localized on most carbon atoms specially atoms of 1,4-dihydropyranopyrazole-5-carbonitrile ring. There is large difference between the negative pole and positive pole formed in compound (12), this difference causes generating large value of dipole moment.

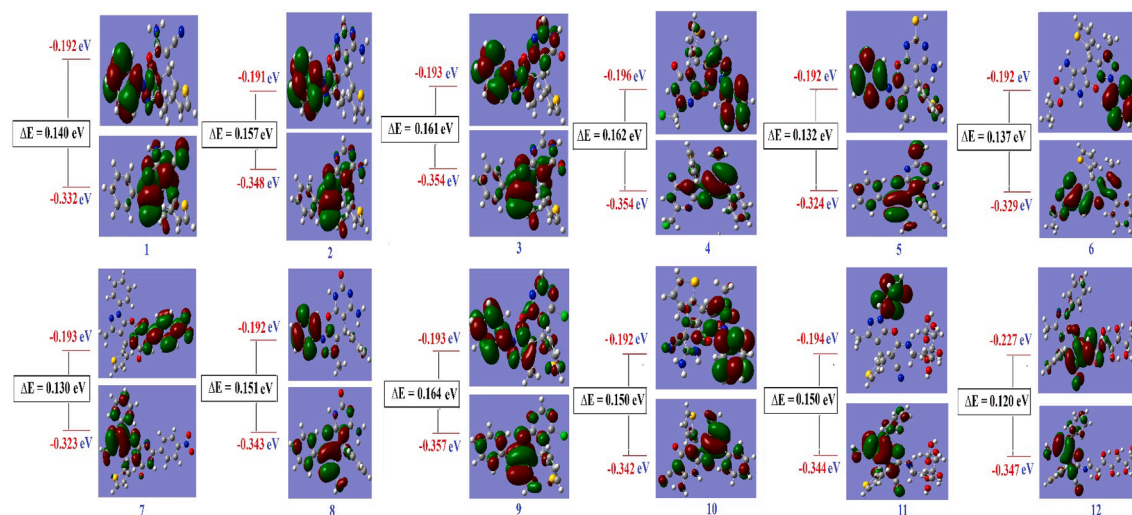


Fig. 14. Molecular orbital surfaces and energy levels of all studied compounds (1–12) by using DFT calculations.

Table 3

Calculated charges on donating sites and energy values (HOMO, LUMO, Energy gap ΔE /eV, hardness (η), global softness (S), electro negativity (χ), absolute softness (σ), chemical potential (Π), global electrophilicity (ω) and additional electronic charge (ΔN_{\max}) of the studied compounds by using DFT calculations.

Parameters	1	2	3	4	5	6	7	8	9	10	11	12
HOMO, H	-0.332	-0.348	-0.354	-0.354	-0.324	-0.329	-0.323	-0.343	-0.357	-0.342	-0.344	-0.347
LUMO, L	-0.192	-0.191	-0.193	-0.196	-0.192	-0.192	-0.193	-0.192	-0.193	-0.192	-0.194	-0.227
I = -H	0.332	0.348	0.354	0.354	0.324	0.329	0.323	0.343	0.357	0.342	0.344	0.347
A = -L	0.192	0.191	0.193	0.196	0.192	0.192	0.193	0.192	0.193	0.192	0.194	0.227
$\Delta E = L - H$	0.140	0.157	0.161	0.162	0.132	0.137	0.130	0.151	0.164	0.150	0.150	0.120
$\eta = (I - A)/2$	0.07	0.079	0.081	0.081	0.066	0.069	0.066	0.076	0.082	0.075	0.075	0.060
$\chi = -(H + L)/2$	0.262	0.269	0.274	0.275	0.258	0.261	0.258	0.268	0.275	0.267	0.269	0.287
$\sigma = 1/\eta$	14.29	12.66	12.35	12.34	15.15	14.49	15.15	13.16	12.19	13.33	13.33	16.67
$S = 1/2\eta$	7.143	6.329	6.173	6.173	7.576	7.246	7.576	6.579	6.098	6.667	6.667	8.333
$\Pi = -\chi$	-0.262	-0.269	-0.274	-0.275	-0.258	-0.261	-0.258	-0.268	-0.275	-0.267	-0.269	-0.287
$\omega = (\Pi)^2/2\eta$	0.490	0.458	0.463	0.467	0.411	0.494	0.504	0.473	0.461	0.475	0.482	0.686
$\Delta N_{\max} = \chi/\eta$	3.743	3.405	3.383	3.395	3.909	4.378	3.909	3.526	3.354	3.560	3.587	4.783

(I) is ionization energy.

(A) is an electron affinity.

3.4. Molecular orbitals and frontier

Molecular orbitals play also an important role in the electric properties, as well as in UV-Vis [51]. An electronic system with smaller values of HOMO-LUMO gap should be more reactive than one having a greater energy gap [44]. The energy gap is closely associated with the reactivity and stability of the executed compounds and shows the nature of the compound with low kinetic stability and slightly high chemical reactivity. On the other hand, the adjacent orbitals are often closely spaced on the frontier region. The energy gap, ΔE of the studied compounds varied between 0.120 for Compound (12) which more reactive and 0.164 eV for compound (9) which less reactive, so electron movement between these orbitals could be easily occur by decreasing the value of energy gap, so that there is a peak around 250 nm in the UV-Vis spectra for all studied compounds.

The nodal properties of molecular orbitals of studied complexes in Fig. 14 are illustrative and suggest orbital delocalization, strong orbital overlap, and low number of nodal planes. The energy difference between HOMO and LUMO (energy gap, ΔE) for the all studied compounds varied according to the type of substitutions as shown in Table 3. All studied chloro compounds (4) and (9) have relatively higher energy gap more than other compounds, so these nitro compounds less reactive. Fig. 14 shows the isodensity surface plots of HOMO and LUMO for the studied compounds. Hard molecules have high the HOMO-LUMO gap, and soft molecules have smaller HOMO-LUMO gap [52]. The values of η and ΔE (HOMO-LUMO) are given in Table 3. It is obvious that the all

studied chloro compounds are hard molecules and η varied from 0.060 for compound (12) to 0.082 for compound (9), also the electronic transition within the compounds is easy as indicated from the ΔE . There are some quantum chemical parameters depending upon the energy values of HOMO and LUMO were calculated as global softness (S), electro negativity (χ), absolute softness (σ), chemical potential (Π), global electrophilicity (ω) and additional electronic charge (ΔN_{\max}) of the all studied compounds. From these values, the compound (9) is absolute soft according to the ($\sigma = 12.19$ eV), while the compound (12) is treated as hard compounds ($\sigma = 16.67$ eV).

As seen in Fig. 14, the all compounds have the same nucleus and different substations, so these compounds are divided into four parts, the 1st part is Pyrano[2,3-c]pyrazole (C1–N9), 2nd part is Thiophen ring (C17–C21), the 3rd part is Phenyl ring (C11–C16), the remaining 4th part is remaining atoms Residual atoms. The electron density of HOMO, Ψ_{87} of the compound (1) is localized mainly on the all atoms of the Pyrano[2,3-c]pyrazole ring with percent 87.6%, with small portion over residual atoms, 12.4%. The LUMO, Ψ_{88} , the electron density localized over all carbon atoms of Phenyl ring in compound (1), with percent (65.1%) and 33.2% on Pyrano[2,3-c]pyrazole, as given in Table 7. Also the HOMO, Ψ_{94} of the compound (2), the electron density localized over all atoms of Pyrano[2,3-c]pyrazole with percent 75.7% and 22.4% on the residual atoms of the compound with small portion on the Phenyl ring, 1.9%. The LUMO, Ψ_{95} of the compound (2), the electron density localized over the phenyl ring with 83.7% and 16.3% on the Pyrano[2,3-c]pyrazole.

Table 4

Computed excitation energies (eV), electronic transition configurations and wave lengths (nm) of the obtained stable compounds; compounds (1–4) by using B3LYP/Cep-31G for the, ($f \geq 0.001$) f = oscillator strengths.

Comp.	eV	nm	Major Contributions	Assignment
1	4.4206	280.48	H-8 \rightarrow L + 5(7%), H-1 \rightarrow L(10%), H \rightarrow L(13%), H-2 \rightarrow L(11%), H-1 \rightarrow L + 3(16%), H \rightarrow L + 1(24%), H \rightarrow L + 3(13%), H-2 \rightarrow L + 3(14%)	π - π^*
	4.2308	293.05	H-8 \rightarrow L(11%), H-8 \rightarrow L + 3(9%), H-7 \rightarrow L(12%), H-7 \rightarrow L + 3(8%), H-7 \rightarrow L + 6(10%), H-6 \rightarrow L(13%), H-6 \rightarrow L + 3(14%)	π - π^*
	4.1772	296.81	H-8 \rightarrow L + 5(12%), H-7 \rightarrow L + 5(8%), H-2 \rightarrow L + 1(11%), H-2 \rightarrow L + 3(13%), H \rightarrow L(24%), H \rightarrow L + 1(23%), H \rightarrow L + 5(14%)	π - π^*
	3.6710	337.74	H-12 \rightarrow L + 5(11%), H-10 \rightarrow L + 5(9%), H-2 \rightarrow L + 5(13%), H \rightarrow L(21%), H \rightarrow L + 2(18%), H \rightarrow L + 5(28%)	n - π^*
2	4.4201	280.5	H-9 \rightarrow L(11%), H-9 \rightarrow L + 4(12%), H-9 \rightarrow L + 5(9%), H-2 \rightarrow L(17%), H \rightarrow L(29%), H \rightarrow L + 2(14%), H \rightarrow L + 4(13%), H \rightarrow L + 5(14%)	π - π^*
	4.3073	287.85	H-10 \rightarrow L + 2(10%), H-7 \rightarrow L(19%), H-7 \rightarrow L + 1(27%), H-7 \rightarrow L + 2(11%), H-7 \rightarrow L + 10(9%), H-6 \rightarrow L + 1(11%), H-6 \rightarrow L + 2(16%)	π - π^*
	4.1549	298.4	H-10 \rightarrow L(7%), H-10 \rightarrow L + 4(10%), H-10 \rightarrow L + 5(8%), H-9 \rightarrow L(12%), H-9 \rightarrow L + 1(11%), H-9 \rightarrow L + 4(6%), H-9 \rightarrow L + 5(7%), H-9 \rightarrow L + 6(11%), H-8 \rightarrow L + 4(13%), H-8 \rightarrow L + 5(11%), H \rightarrow L(24%), H \rightarrow L + 4(18%), H \rightarrow L + 5(14%)	π - π^*
	3.9942	310.41	H-10 \rightarrow L(6%), H-10 \rightarrow L + 10(8%), H-7 \rightarrow L(11%), H-7 \rightarrow L + 1(9%), H-7 \rightarrow L + 2(10%), H-7 \rightarrow L + 4(6%), H-6 \rightarrow L(13%), H-6 \rightarrow L + 1(12%), H-6 \rightarrow L + 4(14%)	n - π^*
3	4.4459	280.01	H-9 \rightarrow L(6%), H-9 \rightarrow L + 1(11%), H-9 \rightarrow L + 3(13%), H-9 \rightarrow L + 4(10%), H-9 \rightarrow L + 5(9%), H-9 \rightarrow L + 6(12%), H-8 \rightarrow L(11%), H-8 \rightarrow L + 1(23%), H-8 \rightarrow L + 3(21%), H-8 \rightarrow L + 4(21%), H-8 \rightarrow L + 5(9%), H-7 \rightarrow L + 1(11%)	π - π^*
	4.3821	282.94	H-10 \rightarrow L(8%), H-3 \rightarrow L(13%), H-2 \rightarrow L(11%), H-2 \rightarrow L + 1(9%), H-1 \rightarrow L(25%), H-1 \rightarrow L + 1(21%), H-1 \rightarrow L + 3(18%), H \rightarrow L(29%), H \rightarrow L + 1(18%), H \rightarrow L + 3(19%)	π - π^*
	4.2592	291.1	H-12 \rightarrow L(14%), H-9 \rightarrow L(11%), H-9 \rightarrow L + 3(12%), H-8 \rightarrow L(6%), H-8 \rightarrow L + 3(29%), H-7 \rightarrow L(19%)	n - π^*
	3.8874	318.94	H-2 \rightarrow L(24%), H-1 \rightarrow L(28%), H \rightarrow L(34%)	π - π^*
	3.4164	362.91	H-6 \rightarrow L(22%), H-6 \rightarrow L + 3(28%), H-6 \rightarrow L + 4(35%), H-6 \rightarrow L + 8(19%)	n - π^*
4	4.4229	280.33	H-9 \rightarrow L(10%), H-9 \rightarrow L + 2(11%), H-9 \rightarrow L + 4(9%), H-8 \rightarrow L + 1(12%), H-8 \rightarrow L(18%), H-8 \rightarrow L + 3(27%), H-8 \rightarrow L + 4(23%), H-8 \rightarrow L + 5(17%), H-8 \rightarrow L + 7(15%), H-7 \rightarrow L + 1(13%)	π - π^*
	4.3639	284.12	H-10 \rightarrow L(8%), H-3 \rightarrow L(13%), H-2 \rightarrow L(19%), H-2 \rightarrow L + 1(21%), H-1 \rightarrow L(19%), H-1 \rightarrow L + 1(25%), H \rightarrow L(20%), H \rightarrow L + 1(9%), H \rightarrow L + 3(10%)	π - π^*
	4.1722	297.17	H-14 \rightarrow L(10%), H-9 \rightarrow L(26%), H-6 \rightarrow L + 3(15%), H-8 \rightarrow L(18%), H-7 \rightarrow L(25%)	n - π^*
	3.8073	325.46	H-2 \rightarrow L(19%), H-1 \rightarrow L(25%), H \rightarrow L(38%)	π - π^*

Table 4 (continued)

Comp.	eV	nm	Major Contributions	Assignment
	3.4165	362.9	H-6 \rightarrow L(24%), H-6 \rightarrow L + 3(29%), H-6 \rightarrow L + 4(18%), H-6 \rightarrow L + 6(12%), H-6 \rightarrow L + 9(13%)	π - π^*

The HOMO of the compound (3), Ψ_{94} , the electron density localized mainly over atoms of Pyrano[2,3-*c*]pyrazole (C1–N9) with percent 78.0.8% and 18.3% on the carbon atoms of residual atoms, also, there is small portion on the phenyl ring (C11–C16) benzene ring (2.9%). The LUMO, Ψ_{95} , the electron density delocalized over all atoms, the most percent (46.1%) is localized on the carbon atoms of phenyl ring (C11–C16). In compound (4), the HOMO, Ψ_{106} , the electron density localized over atoms of the Pyrano[2,3-*c*]pyrazole with percent 77.9%, while the other parts have 19.1% with 0% on thiophen ring. The LUMO, Ψ_{107} , the electron density delocalized over the all atoms with high percent 57.8% on the carbon atoms of phenyl group (C11–C16), 21.7% on the Pyrano[2,3-*c*]pyrazole (C1–N9) and 20.5% on the remaining atoms of thiophen ring and residual atoms. In compound (5), the electron density of HOMO, Ψ_{102} is localized mainly on the hetro atoms, oxygen and nitrogen atoms of the Pyrano[2,3-*c*]pyrazole (C1–N9) with 66.5% and 23.7% on the residual atoms. The LUMO, Ψ_{103} , the electron density localized mainly over all carbon atoms of the phenyl ring (C11–C16) with percent (73.8%) and 26.2% is delocalized on remaining three parts of molecule.

In compound (6), the electron density of HOMO, Ψ_{110} is localized mainly on the carbon and nitrogen atoms of the residual atoms especially on 4,7-dihydro-1H-pyrrol group with percent 79.4%, with small percent 16.9% on the Pyrano[2,3-*c*]pyrazole (C1–N9). The LUMO, Ψ_{111} , the electron density localized over all carbon atoms of the phenyl group (C11–C16) with the most percent (87.8%) and 12.2% is localized on the Pyrano[2,3-*c*]pyrazole (C1–N9). Also the HOMO, Ψ_{125} of the compound (7), the electron density delocalized over all atoms, the most percent (69.8%) is localized on the Pyrano[2,3-*c*]pyrazole (C1–N9) ring, with small portions on phenyl ring 22.9% and 7.3% on the residual atoms. The LUMO, Ψ_{126} , the electron density 86.2% localized mainly with high percent over all atoms of residual atoms with small portion (13.8%) is localized on the Pyrano[2,3-*c*]pyrazole (C1–N9) ring.

The HOMO of the compound (8), Ψ_{98} , the electron density localized mainly over all atoms of Pyrano[2,3-*c*]pyrazole (C1–N9) group with percent (78.5%), with 21.5% spreading over phenyl ring and residual atoms. The LUMO, Ψ_{99} , the electron density localized mainly over all carbon atoms of phenyl ring (C11–C16) with 88.3% and 11.7% localized on Pyrano[2,3-*c*]pyrazole (C1–N9) ring. In compound (9), the HOMO, Ψ_{98} , the electron density delocalized over all atoms of the compound, the most percent (53.7%) is localized on Pyrano[2,3-*c*]pyrazole (C1–N9) ring with small portions on the phenyl ring (27.9%) and 18.4% on the residual atoms. The LUMO, Ψ_{99} , the electron density delocalized over the all atoms with percent (34.2%) on the phenyl ring, 31.5% on the Pyrano[2,3-*c*]pyrazole (C1–N9) and 26.4% on the residual atoms with small portion 7.9% on the thiophen ring (C17–C21).

In compound (10), the electron density of HOMO, Ψ_{104} is localized mainly on the atoms of the Pyrano[2,3-*c*]pyrazole ring with percent 69.3%, 16.8% on the residual atoms with small portion 13.9% on the carbon atoms of phenyl ring (C11–C16). The LUMO, Ψ_{105} , the electron density delocalized over all atoms, specially on the phenyl ring (C11–C16) with 54.3% and Pyrano[2,3-*c*]pyrazole (C1–N9) with 35.9% with small portion 9.8% on the residual atoms. Also the HOMO, Ψ_{134} of the compound (11), the electron density localized over all atoms, the most percent (75.4%) is localized on the Pyrano[2,3-*c*]pyrazole (C1–N9) ring, with small portions on phenyl ring 23.4% and 1.2% on the residual atoms. The LUMO, Ψ_{135} , the electron density 100% localized mainly over all carbon atoms of phenyl ring (C11–C16). The HOMO of the compound (12), Ψ_{138} , the electron density localized mainly over all atoms of Pyrano[2,3-*c*]pyrazole (C1–N9) group with

Table 5

Computed excitation energies (eV), electronic transition configurations and wave lengths (nm) of the obtained stable compounds; compounds (5–8) by using B3LYP/Cep-31G for the, ($f \geq 0.001$) f = oscillator strengths.

Compound	eV	nm	Major Contributions	Assignment
5	4.4509	278.56	H-8 \rightarrow L(11%), H-8 \rightarrow L + 4 (9%), H-8 \rightarrow L + 5(19%), H-1 \rightarrow L + 1(13%), H-1 \rightarrow L + 4(12%), H \rightarrow L(29%), H \rightarrow L + 2(15%), H \rightarrow L + 4(10%), H \rightarrow L + 5 (11%)	π - π^*
	4.3221	286.54	H-8 \rightarrow L (23%), H-8 \rightarrow L + 1 (21%), H-8 \rightarrow L + 2 (19%), H-8 \rightarrow L + 3 (11%), H-8 \rightarrow L + 11 (9%), H-7 \rightarrow L + 1(11%), H-7 \rightarrow L + 2(12%), H-7 \rightarrow L + 3(14%), H-7 \rightarrow L + 11(8%)	π - π^*
	4.1895	295.87	H-11 \rightarrow L (21%), H-11 \rightarrow L + 4 (19%), H-11 \rightarrow L + 5 (2%), H-11 \rightarrow L + 7(9%), H-10 \rightarrow L(13%), H-10 \rightarrow L + 4(11%), H \rightarrow L(7%)	π - π^*
	4.0152	308.78	H-10 \rightarrow L + 5 (11%), H-10 \rightarrow L + 5 (9%), H-2 \rightarrow L + 5 (13%), H \rightarrow L (21%), H \rightarrow L + 2(18%), H \rightarrow L + 5 (28%)	n - π^*
6	4.3844	282.49	H-10 \rightarrow L (24%), H-10 \rightarrow L + 3 (27%), H-10 \rightarrow L + 4 (13%), H-10 \rightarrow L + 5 (12%), H-9 \rightarrow L + 5 (11%)	n - π^*
	3.8476	322.40	H-1 \rightarrow L + 3 (19%), H \rightarrow L (21%), H \rightarrow L + 1 (36%)	π - π^*
	3.6433	340.30	H-7 \rightarrow L (13%), H-7 \rightarrow L + 1 (29%), H-7 \rightarrow L + 3 (18%), H-7 \rightarrow L + 5 (19%), H-7 \rightarrow L + 6 (16%), H-7 \rightarrow L + 8 (22%)	π - π^*
7	6.061	204.57	H-18 \rightarrow L (9%), H-17 \rightarrow L (11%), H-16 \rightarrow L (23%), H-16 \rightarrow L + 1 (7%), H-16 \rightarrow L + 3 (21%), H-16 \rightarrow L + 4 (12%), H-16 \rightarrow L + 7 (14%), H-13 \rightarrow L (12%), H-12 \rightarrow L (22%)	n - π^*
	6.0333	205.5	H-5 \rightarrow L (39%), H-5 \rightarrow L + 1 (24%), H-5 \rightarrow L + 3 (19%)	π - π^*
	4.8813	254.00	H-3 \rightarrow L (10%), H-2 \rightarrow L (23%), H-2 \rightarrow L + 1 (11%), H \rightarrow L (31%), H \rightarrow L + 1 (23%)	π - π^*
	4.7297	262.14	H-7 \rightarrow L (11%), H-7 \rightarrow L + 1 (13%), H-7 \rightarrow L + 3 (12%), H-7 \rightarrow L + 4 (28%), H-7 \rightarrow L + 7 (21%), H-7 \rightarrow L + 10 (10%), H-7 \rightarrow L + 11 (12%), H-7 \rightarrow L + 12 (13%)	n - π^*
	3.9084	317.22	H-14 \rightarrow L (27%), H-14 \rightarrow L + 1 (23%), H-14 \rightarrow L + 3 (18%), H-14 \rightarrow L + 4 (12%), H-14 \rightarrow L + 7 (10%)	n - π^*
	3.1026	399.61	H-11 \rightarrow L (25%), H-11 \rightarrow L + 1 (21%), H-11 \rightarrow L + 3 (15%), H-11 \rightarrow L + 4 (11%), H-11 \rightarrow L + 7 (13%)	n - π^*
8	4.3276	286.5	H-12 \rightarrow L + 8 (12%), H-3 \rightarrow L (10%), H-3 \rightarrow L + 1 (29%), H-3 \rightarrow L + 2 (13%), H-2 \rightarrow L + 1 (24%), H-1 \rightarrow L (15%), H \rightarrow L + 1 (13%)	π - π^*
	4.2169	294.04	H-8 \rightarrow L (22%), H-8 \rightarrow L + 1 (19%), H-8 \rightarrow L + 2 (29%), H-8 \rightarrow L + 4 (12%), H-8 \rightarrow L + 9 (10%), H-5 \rightarrow L + 1 (13%), H-5 \rightarrow L (11%), H-5 \rightarrow L + 1 (10%), H-4 \rightarrow L (9%)	n - π^*
	3.9634	312.82	H \rightarrow L (25%), H \rightarrow L + 1 (23%), H \rightarrow L + 2 (38%)	π - π^*
	3.5556	348.71	H-8 \rightarrow L + 4 (13%), H-8 \rightarrow L + 9 (11%), H-5 \rightarrow L + 2 (27%), H-5 \rightarrow L + 4 (10%), H-5 \rightarrow L + 9	n - π^*

Table 5 (continued)

Compound	eV	nm	Major Contributions	Assignment
			(12%), H-4 \rightarrow L + 2 (11%), H-4 \rightarrow L + 4 (23%), H-4 \rightarrow L + 9 (9%), H-3 \rightarrow L + 4 (11%)	

Table 6

Computed excitation energies (eV), electronic transition configurations and wave lengths (nm) of the obtained stable compounds; compounds (9–12) by using B3LYP/Cep-31G for the, ($f \geq 0.001$) f = oscillator strengths.

Comp.	eV	nm	Major Contributions	Assignment
9	4.4217	280.40	H-4 \rightarrow L + 4(16%), H-2 \rightarrow L + 3 (12%), H-1 \rightarrow L (9%), H-1 \rightarrow L + 1 (12%), H-1 \rightarrow L + 2(10%), H-1 \rightarrow L + 3(13%), H \rightarrow L(21%), H \rightarrow L + 1 (12%), H \rightarrow L + 2(23%)	π - π^*
	4.3591	284.43	H-7 \rightarrow L (12%), H-5 \rightarrow L + 1 (9%), H-2 \rightarrow L (11%), H-1 \rightarrow L (22%), H-1 \rightarrow L + 1 (13%), H-1 \rightarrow L + 2(8%), H-1 \rightarrow L + 5(9%), H \rightarrow L (21%), H \rightarrow L + 1 (7%), H \rightarrow L + 2 (18%), H \rightarrow L + 3 (9%)	π - π^*
	4.2331	292.88	H-12 \rightarrow L (17%), H-9 \rightarrow L + 1 (14%), H-8 \rightarrow L (9%), H-8 \rightarrow L + 1(27%), H-8 \rightarrow L + 2(12%), H-8 \rightarrow L + 9(10%), H-8 \rightarrow L + 10(8%)	n - π^*
	4.0949	302.77	H-9 \rightarrow L (18%), H-8 \rightarrow L (29%), H-8 \rightarrow L + 1 (15%), H-8 \rightarrow L + 2 (16%)	n - π^*
10	6.1091	202.62	H-6 \rightarrow L + 3 (12%), H-5 \rightarrow L + 1 (11%), H-3 \rightarrow L + 1 (13%), H-2 \rightarrow L (29%), H-2 \rightarrow L + 5 (10%), H-1 \rightarrow L + 1 (9%), H \rightarrow L (11%), H \rightarrow L + 2 (12%)	π - π^*
	5.8779	210.95	H-11 \rightarrow L + 6 (13%), H-5 \rightarrow L + 2 (11%), H-2 \rightarrow L + 2 (9%), H \rightarrow L (29%), H \rightarrow L + 1 (21%), H \rightarrow L + 2 (9%)	π - π^*
	5.8161	213.17	H-5 \rightarrow L + 6 (12%), H-2 \rightarrow L + 6 (11%), H-12 \rightarrow L + 6 (13%), H-3 \rightarrow L + 6 (12%), H \rightarrow L + 6 (36%), H-18 \rightarrow L + 6 (11%)	n - π^*
	3.9899	310.74	H-7 \rightarrow L (13%), H-7 \rightarrow L + 1 (14%), H-7 \rightarrow L + 2 (28%), H-7 \rightarrow L + 7 (16%), H-7 \rightarrow L + 8 (12%), H-7 \rightarrow L + 12 (10%)	n - π^*
11	4.4534	278.41	H-20 \rightarrow L + 5 (8%), H-15 \rightarrow L + 5 (13%), H-18 \rightarrow L (21%), H-18 \rightarrow L + 1 (19%), H-18 \rightarrow L + 3 (12%), H-18 \rightarrow L + 8 (9%), H-18 \rightarrow L + 9 (12%), H-4 \rightarrow L + 3 (7%), H-1 \rightarrow L (17%), H-1 \rightarrow L + 1 (13%), H-1 \rightarrow L + 3 (10%), H \rightarrow L + 5 (8%)	π - π^*
	4.2222	293.65	H-8 \rightarrow L + 5 (19%), H-4 \rightarrow L + 1 (14%), H-4 \rightarrow L + 3 (13%), H-2 \rightarrow L (11%), H-2 \rightarrow L + 1 (13%), H \rightarrow L (23%), H \rightarrow L + 1 (21%)	π - π^*
	3.9787	311.62	H-20 \rightarrow L + 5 (11%), H-16 \rightarrow L + 5 (13%), H-15 \rightarrow L + 5 (12%), H-8 \rightarrow L (14%), H-4 \rightarrow L + 5 (11%), H-2 \rightarrow L + 5 (19%), H \rightarrow L (17%)	π - π^*
12	6.0443	205.12	H-16 \rightarrow L (12%), H-13 \rightarrow L + 8 (10%), H-10 \rightarrow L (29%), H \rightarrow L (13%), H \rightarrow L + 7 (24%)	π - π^*
	5.6993	217.54	H-13 \rightarrow L (16%), H-13 \rightarrow L + 4 (18%), H-13 \rightarrow L + 11 (19%), H-10 \rightarrow L + 4 (14%), H \rightarrow L (17%), H \rightarrow L + 7 (13%)	π - π^*
	5.4015	229.54	H-13 \rightarrow L (12%), H-10 \rightarrow L (13%), H-10 \rightarrow L + 4 (17%), H-6 \rightarrow L (22%), H-2 \rightarrow L (11%), H \rightarrow L (37%)	π - π^*

Table 7

Composition of the frontier molecular orbital for studied compounds (1–12) by using DFT/B3LYP/Cep-31G.

	Comp. 1		Comp. 2		Comp. 3		Comp. 4		Comp. 5		Comp. 6	
	H%	L%	H%	L%	H%	L%	H%	L%	H%	L%	H%	L%
Pyrano[2,3-c]pyrazole C1–N9	87.6	33.2	75.7	16.3	78.8	38.2	77.9	21.7	66.5	13.3	16.9	12.2
Thiophen ring C17–C21	0.0	0.0	0.0	0.0	0.0	0.0	0.0	8.6	0.0	11.6	0.0	0.0
Phenyl ring C11–C16	0.0	65.1	1.9	83.7	2.9	46.1	9.7	57.8	9.8	73.8	3.7	87.8
Residual atoms	12.4	1.7	22.4	0.0	18.3	15.7	12.4	11.9	23.7	1.3	79.4	0.0
	Comp. 7		Comp. 8		Comp. 9		Comp. 10		Comp. 11		Comp. 12	
	H%	L%	H%	L%	H%	L%	H%	L%	H%	L%	H%	L%
Pyrano[2,3-c]pyrazole C1–N9	69.8	13.8	78.5	11.7	53.7	31.5	69.3	35.9	75.4	0.0	79.3	83.4
Thiophen ring C17–C21	0.0	0.0	0.0	0.0	0.0	7.9	0.0	0.0	0.0	0.0	0.0	0.0
Phenyl ring C11–C16	22.9	0.0	14.7	88.3	27.9	34.2	13.9	54.3	23.4	100.0	20.7	2.9
Residual atoms	7.3	86.2	6.8	0.0	18.4	26.4	16.8	9.8	1.2	0.0	0.0	13.7

percent (79.3%), with 20.7% spreading over phenyl ring (C11–C16) only. The LUMO, Ψ_{139} , the electron density localized mainly over all carbon atoms of Pyrano[2,3-c]pyrazole with 83.4% and 13.7% localized on the residual atoms with small portion 2.9% on the phenyl ring (C11–C16).

3.5. Excited state

The TD-DFT at the B3LYP level by using G03W program proved to give accurate description of the UV–vis. spectra [53,54]. Time-dependent density functional response theory (TD-DFT) has been recently reformulated [55] to compute discrete transition energies and oscillator strengths and has been applied to a number of different atoms and molecule. Bauernschmitt and Ahlrichs [56] included hybrid functionals proposed in the calculation of the excitation energies. These hybrid methods typically constitute a considerable improvement over conventional Hartree–Fock (HF) based methods. In this work, the optimized geometry was calculated and was used in all subsequent calculations; the wave functions of SCF MOs were explicitly analyzed. The calculated wave functions of the different MOs reflect and suggest the fraction of the different fragments of the complex contributing to the total wave functions of different states. The results indicate, that there is an extent of electron delocalization in the different molecular orbitals.

The electronic transition could be described as a mixed $n \rightarrow \pi^*$ and $\pi \rightarrow \pi^*$ transitions. The energies of HOMO and LUMO states for the all studied compounds are listed in Tables 4–6. The HOMO can perform as an electron donor and the LUMO as the electron acceptor in reaction profile.

Table 4 indicates that there are four excited states are involved in case of compounds (1 and 2). In case of compound (1), 6-amino-3-methyl-1-phenyl-4-(thiophen-2-yl)-1,4-dihydropyran[2,3-c]pyrazole-5-carbonitrile, the first excited state results from a combination eight transitions, H-8 \rightarrow L + 5 (7%), H-1 \rightarrow L (10%), H \rightarrow L (13%), H-2 \rightarrow L (11%), H-1 \rightarrow L + 3 (16%), H \rightarrow L + 1 (24%), H \rightarrow L + 3 (13%), H-2 \rightarrow L + 3 (14%), this excited state assigned to $\pi\text{-}\pi^*$ at 280.48 nm and 4.4206 eV. The second excited state result from interaction between electronic configurations, which represent $\pi \rightarrow \pi^*$ transition. This is transition results from H-8 \rightarrow L (11%), H-8 \rightarrow L + 3 (9%), H-7 \rightarrow L (12%), H-7 \rightarrow L + 3 (8%), H-7 \rightarrow L + 6 (10%), H-6 \rightarrow L (13%), H-6 \rightarrow L + 3 (14%) and can be observed around 293.05 nm and 4.2308 eV. The third excited state is assigned to $\pi \rightarrow \pi^*$ transition, represents a transition appears at 296.81 nm and 4.1772 eV, H-8 \rightarrow L + 5 (12%), H-7 \rightarrow L + 5 (8%), H-2 \rightarrow L + 1 (11%), H-2 \rightarrow L + 3 (13%), H \rightarrow L (24%), H \rightarrow L + 1 (23%), H \rightarrow L + 5 (14%). The fourth excited state at 337.74 nm and 3.6710 eV, results as

H-12 \rightarrow L + 5 (11%), H-10 \rightarrow L + 5 (9%), H-2 \rightarrow L + 5 (13%), H \rightarrow L (21%), H \rightarrow L + 2 (18%), H \rightarrow L + 5 (28%) and assigned to $n\text{-}\pi^*$. Also, in compound (2), 3-methyl-1-phenyl-4-(thiophen-2-yl)-1,4-dihydropyrazolo[4',3':5,6]pyrano[2,3-d]pyrimidin-5-amine, the first excited state assigned to an $\pi \rightarrow \pi^*$ transition at 280.5 nm and 4.4201 eV, this transition represented by H-9 \rightarrow L (11%), H-9 \rightarrow L + 4 (12%), H-9 \rightarrow L + 5 (9%), H-2 \rightarrow L (17%), H \rightarrow L (29%), H \rightarrow L + 2 (14%), H \rightarrow L + 4 (13%), H \rightarrow L + 5 (14%). The second excited state is assigned to $\pi \rightarrow \pi^*$ transitions, represents a transitions H-10 \rightarrow L + 2 (10%), H-7 \rightarrow L (19%), H-7 \rightarrow L + 1 (27%), H-7 \rightarrow L + 2 (11%), H-7 \rightarrow L + 10 (9%), H-6 \rightarrow L + 1 (11%), H-6 \rightarrow L + 2 (16%) which observed around 287.85 nm and 4.3073 eV. The third excited state is assigned to $\pi \rightarrow \pi^*$ transition, represents a transition appears at 298.4 nm and 4.1549 eV, H-10 \rightarrow L (7%), H-10 \rightarrow L + 4 (10%), H-10 \rightarrow L + 5 (8%), H-9 \rightarrow L (12%), H-9 \rightarrow L + 1 (11%), H-9 \rightarrow L + 4 (6%), H-9 \rightarrow L + 5 (7%), H-9 \rightarrow L + 6 (11%), H-8 \rightarrow L + 4 (13%), H-8 \rightarrow L + 5 (11%), H \rightarrow L (24%), H \rightarrow L + 4 (18%), H \rightarrow L + 5 (14%). The fourth excited state at 310.41 nm and 3.9942 eV, results as H-10 \rightarrow L (6%), H-10 \rightarrow L + 10 (8%), H-7 \rightarrow L (11%), H-7 \rightarrow L + 1 (9%), H-7 \rightarrow L + 2 (10%), H-7 \rightarrow L + 4 (6%), H-6 \rightarrow L (13%), H-6 \rightarrow L + 1 (12%), H-6 \rightarrow L + 4 (14%) and assigned to $n\text{-}\pi^*$.

In compounds (3 and 4), there are five transitions can be observed as given in Table 4. In compound (3), 3-methyl-1-phenyl-4-(thiophen-2-yl)-4,6-dihydropyrazolo [4',3':5,6]pyrano[2,3-d]pyrimidin-5(1H)-one, the first excited state can be appeared at 280.01 nm and 4.4459 eV, which results from H-9 \rightarrow L (6%), H-9 \rightarrow L + 1 (11%), H-9 \rightarrow L + 3 (13%), H-9 \rightarrow L + 4 (10%), H-9 \rightarrow L + 5 (9%), H-9 \rightarrow L + 6 (12%), H-8 \rightarrow L (11%), H-8 \rightarrow L + 1 (23%), H-8 \rightarrow L + 3 (21%), H-8 \rightarrow L + 4 (21%), H-8 \rightarrow L + 5 (9%), H-7 \rightarrow L + 1 (11%), this assigned to $\pi\text{-}\pi^*$. The second excited state can be observed at 282.94 nm and 4.3821 eV, results as H-10 \rightarrow L (8%), H-3 \rightarrow L (13%), H-2 \rightarrow L (11%), H-2 \rightarrow L + 1 (9%), H-1 \rightarrow L (25%), H-1 \rightarrow L + 1 (21%), H-1 \rightarrow L + 3 (18%), H \rightarrow L (29%), H \rightarrow L + 1 (18%), H \rightarrow L + 3 (19%), this assigned to $\pi\text{-}\pi^*$. The third excited state results from H-12 \rightarrow L (14%), H-9 \rightarrow L (11%), H-9 \rightarrow L + 3 (12%), H-8 \rightarrow L (6%), H-8 \rightarrow L + 3 (29%), H-7 \rightarrow L (19%), this assigned to $n\text{-}\pi^*$ transition and can be observed at 291.1 nm. The fourth excited state can be obtained at 318.94 nm and 3.8874 eV, this transition results from H-2 \rightarrow L (24%), H-1 \rightarrow L (28%), H \rightarrow L (34%). Finally, the fifth transition state observed at 362.91 nm and 3.4164 eV and assigned to $n\text{-}\pi^*$ transition can be obtained from H-6 \rightarrow L (22%), H-6 \rightarrow L + 3 (28%), H-6 \rightarrow L + 4 (35%), H-6 \rightarrow L + 8 (19%). These values of electronic transitions agree nicely with the experimental measurements. In compound (4), 7-(chloromethyl)-3-methyl-1-phenyl-4-(thiophen-2-yl)-4,6-dihydropyrazolo[4',3':5,6] pyrano[2,3-d]pyrimidin-5(1H)-one, the first excited state can be appeared at 280.33 nm and 4.4229 eV, which results from

Table 8

In vitro anti-inflammatory activity of the newly synthesized compounds compared to standard celecoxib and quercetin.

Groups	Cox-1 ($\mu\text{M IC}_{50}$)	Cox-2 ($\mu\text{M IC}_{50}$)	Selectivity index (COX-1/COX-2)	LOX ($\mu\text{M IC}_{50}$)
Celecoxib	14.60 \pm 0.00 ^f	0.04 \pm 0.00 ^a	365	
Quercetin				3.35 \pm 0.01 ^d
Compound 1	5.47 \pm 0.12 ^a	0.25 \pm 0.00 ^d	21.88	4.43 \pm 0.15 ^f
Compound 4	10.67 \pm 0.16 ^c	0.06 \pm 0.00 ^b	177.83	3.00 \pm 0.06 ^e
Compound 8	7.63 \pm 0.06 ^b	0.18 \pm 0.01 ^c	42.39	3.90 \pm 0.10 ^e
Compound 11	14.23 \pm 0.15 ^e	0.04 \pm 0.00 ^a	355.75	2.17 \pm 0.12 ^a
Compound 12	13.43 \pm 0.15 ^d	0.04 \pm 0.00 ^a	335.75	2.53 \pm 0.06 ^b

H-9 \rightarrow L (10%), H-9 \rightarrow L + 2 (11%), H-9 \rightarrow L + 4 (9%), H-8 \rightarrow L + 1 (12%), H-8 \rightarrow L (18%), H-8 \rightarrow L + 3 (27%), H-8 \rightarrow L + 4 (23%), H-8 \rightarrow L + 5 (17%), H-8 \rightarrow L + 7 (15%), H-7 \rightarrow L + 1 (13%), this assigned to π - π^* . The second excited state can be observed at 284.12 nm and 4.3639 eV, results as H-10 \rightarrow L (8%), H-3 \rightarrow L (13%), H-2 \rightarrow L (19%), H-2 \rightarrow L + 1 (21%), H-1 \rightarrow L (19%), H-1 \rightarrow L + 1 (25%), H \rightarrow L (20%), H \rightarrow L + 1 (9%), H \rightarrow L + 3 (10%), this assigned to π - π^* . The third excited state results from H-14 \rightarrow L (10%), H-9 \rightarrow L (26%), H-6 \rightarrow L + 3 (15%), H-8 \rightarrow L (18%), H-7 \rightarrow L (25%), this assigned to n- π^* transition and can be observed at 297.17 nm. The fourth excited state can be obtained at 325.46 nm and 3.8073 eV, this transition results from H-2 \rightarrow L (19%), H-1 \rightarrow L (25%), H \rightarrow L (38%). The fifth transition state observed at 362.9 nm and 3.4165 eV and assigned to π - π^* transition can be obtained from H-6 \rightarrow L (24%), H-6 \rightarrow L + 3 (29%), H-6 \rightarrow L + 4 (18%), H-6 \rightarrow L + 6 (12%), H-6 \rightarrow L + 9 (13%). These values of electronic transitions agree nicely with the experimental data obtained from Uv-Vis measurements.

In Table 5, the number of excited states involved in compounds (5–8) are given, in compound (5), 5-amino-3-methyl-1-phenyl-4-(thiophen-2-yl)-1,4-dihydropyrazolo [4',3':5,6]pyrano[2,3-d]pyrimidine-7-thiol, there are four excited states, three of them are assigned to π - π^* transition and can be observed at 278.56, 286.54, 295.87 nm, respectively and one is assigned to n- π^* transition, which can be observed at 308.78 nm. In compound (6), Ethyl 5-amino-3-methyl-1-phenyl-4-(thiophen-2-yl)-4,7-dihydro-1H-pyrrolo[3',2':5,6]pyrano[2,3-c]pyrazole-6-carboxylate, there are three of excited states can be occurred, the first one is assigned to n- π^* transition at 282.49 nm, while second and third assigned to π - π^* and can be observed at 322.40 nm and 340.30 nm. In case of compound (7), 3-methyl-7-(4-nitrophenyl)-1-phenyl-4-(thiophen-2-yl)-4,6,7,8-tetrahydropyrazolo[4',3':5,6]pyrano[2,3-d]pyrimidin-5(1H)-one, there are six excited states can be observed, four of them are assigned to n- π^* transition and can be observed at 204.57, 262.14, 317.22 and 399.61 nm, while there are two excited states are assigned to π - π^* which can be observed at 205.5 and 254.00 nm. These values of electronic transitions agree nicely with the experimental measurements. There are four excited states can be obtained in case of compound (8), 5-amino-3-methyl-1-phenyl-4-(thiophen-2-yl)-4,8-dihydropyrazolo[4',3':5,6]pyrano[2,3-b]pyridin-7(1H)-one, two of them are assigned to π - π^* transition, 286.5 and 312.82 nm and others assigned to n- π^* transition and can be observed at 294.04 and 348.71 nm.

The electronic transition configurations and wave lengths for compounds (9–12) are given in Table 6. For compound (9), 5-chloro-3-methyl-1-phenyl-4-(thiophen-2-yl)-1,4-dihydropyrazolo[4',3':5,6]pyrano[2,3-d]pyrimidine, there are four excited states, the first and second of them are assigned to π - π^* transition and the others of them, third and fourth are assigned to n- π^* transition. the π - π^* transitions can be observed at 280.40 and 284.43 nm, while the n- π^* transitions can be observed at 292.88 and 302.77 nm. These values of electronic transitions agree nicely with the experimental measurements. In compound (10), 7-amino-3-methyl-5-oxo-1-phenyl-4-(thiophen-2-yl)-1,4,5,8-tetrahydropyrazolo[4',3':5,6]pyrano[2,3-b]pyridine-6-carbonitrile, there are four excited states, two of them can be observed at 202.62 and 210.95 nm, these values assigned to π - π^* transitions, while the others can be appeared at 213.17 and 310.74 nm, these transitions are assigned to n- π^* transitions. While, compound (11), 3-methyl-6-(((2R,3S,4S,5R,6R)-2,3,4,5,6-pentahydroxytetrahydro-2H-pyran-2-yl)

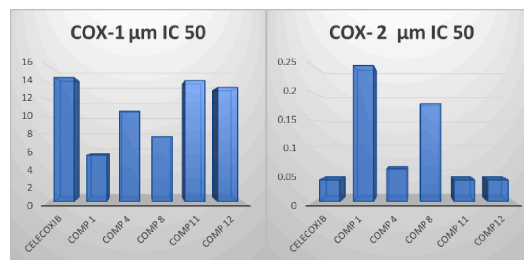


Fig. 15. A statistical representation for the COX-1 and COX-2 enzymes inhibitory activity of newly synthesized compounds.

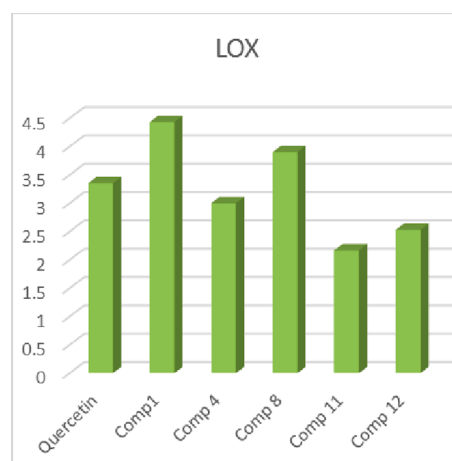


Fig. 16. A statistical representation for the LOX enzyme inhibitory activity of newly synthesized compounds.

methylamino)-1-phenyl-4-(thiophen-2-yl)-1,4-dihydropyran[2,3-c]pyrazole-5-carbonitrile, there are three electronic transition can be occurred at 278.41, 293.65 and 311.62 nm. All of these transition are assigned to π - π^* transitions, there is no any n- π^* transition involved. Also, the transitions of compound (12) 3-methyl-6-(((2S,3S,4S,5R,E)-2,3,4,5,6-pentahydroxy hexylidene)amino)-1-phenyl-4-(thiophen-2-yl)-1,4-dihydropyran[2,3-c] pyrazole-5-carbonitrile, free from n- π^* transitions. There are three excited states can be observed at 205.12, 217.54 and 229.54 nm, all of these transitions are assigned to π - π^* transitions.

3.6. Pharmacology

3.6.1. In vitro anti-inflammatory screening

Cyclooxygenases (COX) are responsible for the formation of prostanooids as thromboxane and prostaglandins. COX inhibitors can relieve the symptoms of inflammation and pain [57]. All the newly synthesized compounds inhibit both cyclooxygenase and lipoxygenase enzymes. Compounds 1 and 8 inhibit Cox –1 more than the standard celecoxib in 5.47 \pm 0.12 and 7.63 \pm 0.06 $\mu\text{M IC}_{50}$ respectively, in comparison to 14.60 \pm 0.00 of the standard celecoxib. Concerning Cox-2, Compounds

Table 9
In vitro total antioxidant activity of the newly synthesized compounds.

Groups	Total antioxidant (IC ₅₀ U/ML)
Ascorbic acid	29.40 ± 0.62 ^d
Compound 1	22.26 ± 0.15 ^a
Compound 4	26.57 ± 0.15 ^c
Compound 8	24.27 ± 0.14 ^b
Compound 11	44.93 ± 0.15 ^f
Compound 12	39.60 ± 0.10 ^e

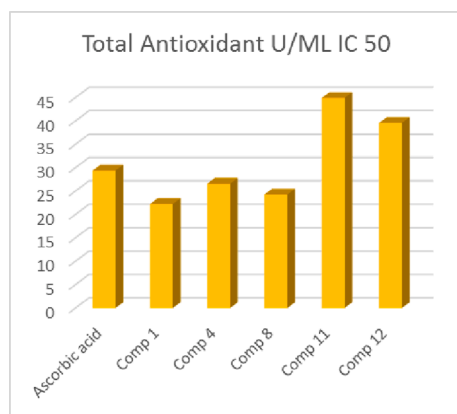


Fig. 17. A statistical representation for the antioxidant activity of the newly prepared compound.

11 and **12** are more potent than other compounds in reducing their activity. They also inhibit lipoxygenase enzyme to 2.17 ± 0.12 and $2.53 \pm 0.06 \mu\text{m}$, respectively, in comparison to 3.35 ± 0.01 of the standard quercetin. In conclusion, compounds **11** and **12** have more anti-inflammatory activity than other compounds as their COX-1/COX-2 selectivity index are 335.75 and 355.75, respectively, compared to 21.88, 177.83, and 42.39 for compounds 1,4 and 8, respectively (Table 8) (Figs. 15, 16).

Different superscript letters in the same column are significantly different at $p \geq 0.05$. Values are expressed as mean \pm SD ($n = 3$).

The obtained results revealed that these compounds have a dual mechanism of action as they inhibit both COX and 5-LOX to be novel compounds to treat inflammation. They act by blocking both prostaglandins and leukotrienes formation. This dual mechanism of action could be helpful for the management of both pain and inflammation pathways. The sugar content of compounds 11 and 12 explained their superior anti-inflammatory activity than other compounds. In this concern, [58] reported that ibuprofen sugar derivatives showed better anti-inflammatory activity and enhanced bioavailability. Other researchers reported that newly synthesized pyranopyrazole compounds exhibited anti-inflammatory activity and COX-1/2 inhibition [59] while Kumar et al. [60] validated the use of pyranopyrazole compounds as anti-inflammatory via docking studies. Also, the newly synthesized compounds could be promising in the treatment of hepatocellular carcinoma as recent studies demonstrated that COX-2 inhibitors decrease the immunosuppressive transforming growth factor-beta (TGF β) expression in hepatocytes and consequently inhibit epithelial-mesenchymal transition (EMT) [61].

3.6.2. In vitro antioxidant activity screening

Antioxidants are essential to relieve the oxidative stress, production of reactive oxygen species and subsequently decrease several diseases' pathogenesis. It also prevents necrosis and or apoptosis [62,63]. TAC is an analyte frequently used to evaluate the antioxidant response against the free radicals produced. Low total antioxidant capacity could be indicative of oxidative stress or increased susceptibility to oxidative

damage. Results indicated that compounds **11** and **12** exhibited significant ($p \geq 0.05$) in vitro total antioxidant activity as 44.93 ± 0.15 and 39.60 ± 0.10 U/ML, respectively higher than standard ascorbic acid (29.40 ± 0.62). (Table 9) (Fig. 17).

4. Conclusion

The authors herein endeavored to design an efficient and environmentally friendly protocol developed to synthesize 1,4-dihydropyran [2,3-c]pyrazole-5-carbonitrile (**1**) by the one-pot three-component condensation reaction carried out by the reaction of 5-methyl-2-phenyl-2,4-dihydro-3H-pyrazol-3-one, thiophene-2-carbaldehyde, and malononitrile. The start compound is used to obtain polycyclic heterocyclic systems. In addition, The newly synthesized compounds

were found to be potent towards the antioxidant activity. Results indicated that compounds **11** and **12** in vitro total antioxidant activity were higher than those of standard ascorbic acid.

Declaration of Competing Interest

The authors declare that they have no known competing financial interests or personal relationships that could have appeared to influence the work reported in this paper.

Acknowledgments

The authors are very thankful to Taif University Researches Supporting Project Number (TURSP-2020/91), Taif University, Taif, Saudi Arabia.

References

- [1] Y. Gu, Multicomponent reactions in unconventional solvents: state of the art, *Green Chem.* 14 (2012) 2091–2128, <https://doi.org/10.1039/C2GC35635J>.
- [2] E. Ruijter, R. Scheffelaar, R.V. Orru, Multicomponent reaction design in the quest for molecular complexity and diversity, *Angew. Chem. Int. Ed.* 50 (2011) 6234–6246, <https://doi.org/10.1002/anie.201006515>.
- [3] A. Shaabani, S.E. Hooshmand, Malononitrile dimer as a privileged reactant in design and skeletal diverse synthesis of heterocyclic motifs, *Mol. Diversity* 22 (2018) 207–224, <https://doi.org/10.1007/s11030-017-9807-y>.
- [4] P. Verma, S. Pal, S. Chauhan, A. Mishra, I. Sinha, S. Singh, V. Srivastava, Starch functionalized magnetite nanoparticles: a green, biocatalyst for one-pot multicomponent synthesis of imidazopyrimidine derivatives in aqueous medium under ultrasound irradiation, *J. Mol. Struct.* 1203 (2020) 127410, <https://doi.org/10.1016/j.molstruc.2019.127410>.
- [5] N. Narayan, A. Meiyazhagan, R. Vajtai, Metal nanoparticles as green catalysts, *Materials* 12 (2019) 3602, <https://doi.org/10.3390/ma12213602>.
- [6] K. Eskandari, B. Karami, S. Khodabakhshi, ZnO nanoparticles—a recyclable catalyst for the synthesis of bis (pyrazolyl) methanes, *Chem. Heterocycl. Compd.* 50 (2015) 1658–1664, <https://doi.org/10.1007/s10593-015-1635-3>.
- [7] M. Bakherad, A. Keivanloo, M. Gholizadeh, R. Doosti, M. Javanmardi, Using magnetized water as a solvent for a green, catalyst-free, and efficient protocol for the synthesis of pyrano [2, 3-c] pyrazoles and pyrano [4', 3': 5, 6] pyrazolo [2, 3-d] pyrimidines, *Res. Chem. Intermed.* 43 (2017) 1013–1029, <https://doi.org/10.1007/s11164-016-2680-y>.
- [8] A. Mandour, E. El-Sawy, M. Ebad, S. Hassan, Synthesis and potential biological activity of some novel 3-[(N-substituted indol-3-yl) methyleneamino]-6-amino-4-aryl-pyrano (2, 3-c) pyrazole-5-carbonitriles and 3, 6-diamino-4-(N-substituted indol-3-yl) pyrano (2, 3-c) pyrazole-5-carbonitriles, *Acta Pharmaceutica* 62 (2012) 15–30, <https://doi.org/10.2478/v10007-012-0007-0>.
- [9] N. Foloppe, L.M. Fisher, R. Howes, A. Potter, A.G. Robertson, A.E. Surgenor, Identification of chemically diverse Chk1 inhibitors by receptor-based virtual screening, *Bioorg. Med. Chem.* 14 (2006) 4792–4802, <https://doi.org/10.1016/j.bmc.2006.03.021>.
- [10] N.J. Thumar, M.P. Patel, Synthesis and in vitro antimicrobial evaluation of 4H-pyrazolopyran-, benzopyran and naphthopyran derivatives of 1H-pyrazole, *Arxivoc* 13 (2009) 363–380.
- [11] F.M. Abdelrazek, P. Metz, N.H. Metwally, S.F. El-Mahrouky, Synthesis and molluscicidal activity of new cinnoline and pyrano [2, 3-c] pyrazole derivatives, *Archiv der Pharmazie: Int. J. Pharmac. Med. Chem.* 339 (2006) 456–460, <https://doi.org/10.1002/ardp.200600057>.
- [12] M.E. Zaki, H.A. Soliman, O.A. Hiekal, A.E. Rashad, Pyrazolopyranopyrimidines as a class of anti-inflammatory agents, *Zeitschrift für Naturforschung C* 61 (2006) 1–5, <https://doi.org/10.1515/znc-2006-1-201>.
- [13] A. Tanitame, Y. Oyamada, K. Ofuji, M. Fujimoto, N. Iwai, Y. Hiyama, K. Suzuki, H. Ito, H. Terauchi, M. Kawasaki, Synthesis and antibacterial activity of a novel

- series of potent DNA gyrase inhibitors. Pyrazole derivatives, *J. Med. Chem.* 47 (2004) 3693–3696, <https://doi.org/10.1021/jm030394f>.
- [14] H. Mecadon, M.R. Rohman, I. Kharbanger, B.M. Laloo, I. Kharkongor, M. Rajbangshi, B. Myrbo, L-Proline as an efficient catalyst for the multi-component synthesis of 6-amino-4-alkyl/aryl-3-methyl-2, 4-dihydropyran [2, 3-c] pyrazole-5-carbonitriles in water, *Tetrahedron Lett.* 52 (2011) 3228–3231, <https://doi.org/10.1016/j.tetlet.2011.04.048>.
- [15] M. Hogale, B. Pawar, Synthesis and Biological Activity of 1-Aroyl-5-(p-sulfamoyl-phenylazo)-3, 4-dimethylpyran (2, 3-c) pyrazol-6 (1H)-ones, *ChemInform* 21 (1990) <https://doi.org/10.1002/chin.199004162>.
- [16] K. Saravana Mani, S.P. Rajendran, L-Proline catalyzed three component synthesis of pyrano [2, 3-c] pyrazole-5-carbonitrile derivatives and in vitro antimalarial evaluation, *Synth. Commun.* 47 (2017) 2036–2043, <https://doi.org/10.1080/00397911.2017.1362437>.
- [17] N.K. Bejjanki, A. Venkatesham, J. Madda, N. Kommu, S. Pombala, C.G. Kumar, K. R. Prasad, J.B. Nanubolu, Synthesis of new chromeno-annulated cis-fused pyrano [4, 3-c] isoxazole derivatives via intramolecular nitrene cycloaddition and their cytotoxicity evaluation, *Bioorg. Med. Chem. Lett.* 23 (2013) 4061–4066, <https://doi.org/10.1039/C2MD20023F>.
- [18] S.R. Mandha, S. Siliveri, M. Alla, V.R. Bommena, M.R. Bommineni, S. Balasubramanian, Eco-friendly synthesis and biological evaluation of substituted pyrano [2, 3-c] pyrazoles, *Bioorg. Med. Chem. Lett.* 22 (2012) 5272–5278, <https://doi.org/10.1016/j.bmcl.2012.06.055>.
- [19] Z. Mahmoudi, M.A. Ghasemzadeh, H. Kabiri-Fard, Fabrication of UiO-66 nanocages confined brønsted ionic liquids as an efficient catalyst for the synthesis of dihydropyrazolo [4', 3': 5, 6] pyrano [2, 3-d] pyrimidines, *J. Mol. Struct.* 1194 (2019) 1–10, <https://doi.org/10.1016/j.molstruc.2019.05.079>.
- [20] X.-H. Yang, P.-H. Zhang, Z.-M. Wang, F. Jing, Y.-H. Zhou, L.-H. Hu, Synthesis and bioactivity of lignin related high-added-value 2H, 4H-dihydro-pyrano [2, 3-c] pyrazoles and 1H, 4H-dihydro-pyrano [2, 3-c] pyrazoles, *Ind. Crops Prod.* 52 (2014) 413–419, <https://doi.org/10.1016/j.indcrop.2013.11.017>.
- [21] H. Kashtoh, M.T. Muhammad, J.J. Khan, S. Rasheed, A. Khan, S. Perveen, K. Javaid, K.M. Khan, M.I. Choudhary, Dihydropyran [2, 3-c] pyrazole: novel in vitro inhibitors of yeast α -glucosidase, *Bioorg. Chem.* 65 (2016) 61–72, <https://doi.org/10.1016/j.bioorg.2016.01.008>.
- [22] S.C. Kuo, L.J. Huang, H. Nakamura, Studies on heterocyclic compounds. 6. Synthesis and analgesic and antiinflammatory activities of 3, 4-dimethylpyrano [2, 3-c] pyrazol-6-one derivatives, *J. Med. Chem.* 27 (1984) 539–544, <https://doi.org/10.1021/jm00370a020>.
- [23] L. Rodinovskaya, A. Gromova, A. Shestopalov, V. Nesterov, Synthesis of 6-amino-4-aryl-5-cyano-3-(3-cyanopyridin-2-ylthiomethyl)-2, 4-dihydropyran [2, 3-c] pyrazoles and their hydrogenated analogs. Molecular structure of 6-amino-5-cyano-3-(3-cyano-4, 6-dimethylpyridin-2-ylthiomethyl)-4-(2-nitrophenyl)-2, 4-dihydropyran [2, 3-c] pyrazole, *Russian Chem. Bull.* 52 (2003) 2207–2213, <https://doi.org/10.1023/B:RUCB.0000011880.05561.c1>.
- [24] X.-T. Li, A.-D. Zhao, L.-P. Mo, Z.-H. Zhang, Meglumine catalyzed expeditious four-component domino protocol for synthesis of pyrazolopyranopyrimidines in aqueous medium, *RSC Adv.* 4 (2014) 51580–51588, <https://doi.org/10.1039/C4RA08689A>.
- [25] B. Maleki, S.S. Ashrafi, Nano α -Al₂O₃ supported ammonium dihydrogen phosphate (NH₄ H₂P₂O₄/A₂O₃): preparation, characterization and its application as a novel and heterogeneous catalyst for the one-pot synthesis of tetrahydrobenzo [b] pyran and pyrano [2, 3-c] pyrazole derivatives, *RSC Adv.* 4 (2014) 42873–42891, <https://doi.org/10.1039/C4RA07813F>.
- [26] C. Derabli, I. Boualia, A.B. Abdelwahab, R. Boulcina, C. Bensouici, G. Kirsch, A. Debache, A cascade synthesis, in vitro cholinesterases inhibitory activity and docking studies of novel Tacrine-pyranopyrazole derivatives, *Bioorg. Med. Chem. Lett.* 28 (2018) 2481–2484, <https://doi.org/10.1016/j.bmcl.2018.05.063>.
- [27] I. Gameiro, P. Michalska, G. Tenti, A. Cores, I. Buendia, A.I. Rojo, N. D. Georgakopoulos, J.M. Hernández-Guijo, M.T. Ramos, G. Wells, Discovery of the first dual GSK3 β inhibitor/Nrf2 inducer. A new multitarget therapeutic strategy for Alzheimer's disease, *Sci. Rep.* 7 (2017) 1–15, <https://doi.org/10.1038/srep45701>.
- [28] M.R. Tipale, L.D. Killare, A.R. Deshmukh, M.R. Bhosle, An efficient four component domino synthesis of pyrazolopyranopyrimidines using recyclable choline chloride: urea deep eutectic solvent, *J. Heterocycl. Chem.* 55 (2018) 716–728, <https://doi.org/10.1002/jhet.3095>.
- [29] L. Chen, H. Deng, H. Cui, J. Fang, Z. Zuo, J. Deng, Y. Li, X. Wang, L. Zhao, Inflammatory responses and inflammation-associated diseases in organs, *Oncotarget* 9 (2018) 7204, <https://doi.org/10.18632/oncotarget.23208>.
- [30] W.S. Shehab, W.H. El-Shwiniy, Nanoparticles of manganese oxides as efficient catalyst for the synthesis of pyrano [2, 3-d] pyrimidine derivatives and their complexes as potent protease inhibitors, *J. Iran. Chem. Soc.* 15 (2018) 431–443, <https://doi.org/10.1007/s13738-017-1244-4>.
- [31] W.S. Shehab, G.T. El-Bassyouni, Synthesis and cyclization of β -keto-enol derivatives tethered indole and pyrazole as potential antimicrobial and anticancer activity, *J. Iran. Chem. Soc.* 15 (2018) 1639–1645, <https://doi.org/10.1007/s13738-018-1362-7>.
- [32] M.H. Abdel-Azim, M.A. Aziz, S.M. Mouneir, A.F. EL-Faragy, W.S. Shehab, Ecofriendly synthesis of pyrano [2, 3-d] pyrimidine derivatives and related heterocycles with anti-inflammatory activities, *Archiv der Pharmazie* 353 (2020) 2000084, <https://doi.org/10.1002/ardp.202000084>.
- [33] W.S. Shehab, M.H. Abdellattif, S.M. Mouneir, Heterocyclization of polarized system: synthesis, antioxidant and anti-inflammatory 4-(pyridin-3-yl)-6-(thiophen-2-yl) pyrimidine-2-thiol derivatives, *Chem. Cent. J.* 12 (2018) 1–8, <https://doi.org/10.1186/s13065-018-0437-y>.
- [34] M.M. Amer, M.A. Aziz, W.S. Shehab, M.H. Abdellattif, S.M. Mouneir, Recent Advances in chemistry and pharmacological aspects of 2-pyridone scaffolds, *J. Saudi Chem. Soc.* 25 (2021) 101259, <https://doi.org/10.1016/j.jscs.2021.101259>.
- [35] W.H. El-Shwiniy, W.S. Shehab, W.A. Zordok, Spectral, thermal, DFT calculations, anticancer and antimicrobial studies for bivalent manganese complexes of pyrano [2, 3-d] pyrimidine derivatives, *J. Mol. Struct.* 1199 (2020) 126993, <https://doi.org/10.1016/j.molstruc.2019.126993>.
- [36] M.J. Frisch, Gaussian 98, Revision A. 9, 1998.
- [37] W. Kohn, Density functional and density matrix method scaling linearly with the number of atoms, *Phys. Rev. Lett.* 76 (1996) 3168, <https://doi.org/10.1103/PhysRevLett.76.3168>.
- [38] A.D. Becke, Density-functional exchange-energy approximation with correct asymptotic behavior, *Phys. Rev. A* 38 (1988) 3098, <https://doi.org/10.1103/PhysRevA.38.3098>.
- [39] C. Lee, W. Yang, R.G. Parr, Development of the Colle-Salvetti correlation-energy formula into a functional of the electron density, *Phys. Rev. B* 37 (1988) 785, <https://doi.org/10.1103/PhysRevB.37.785>.
- [40] R.L. Flurry, Molecular orbital theories of bonding in organic molecules, 1968.
- [41] R.H. Crabtree, Recent developments in the organometallic chemistry of N-heterocyclic carbenes, *Coord. Chem. Rev.* 5 (2007) 595.
- [42] S. Top, J. Tang, A. Vessieres, C. Carrez, C. Provot, G. Jaouen, *Chem. Commun. (J. Chem. Soc. Sect. D)* (1996) 955–956.
- [43] A. Siddekha, A. Nizam, M. Pasha, An efficient and simple approach for the synthesis of pyranopyrazoles using imidazole (catalytic) in aqueous medium, and the vibrational spectroscopic studies on 6-amino-4-(4'-methoxyphenyl)-5-cyano-3-methyl-1-phenyl-1, 4-dihydropyran [2, 3-c] pyrazole using density functional theory, *Spectrochim. Acta Part A Mol. Biomol. Spectrosc.* 81 (2011) 431–440, <https://doi.org/10.1016/j.saa.2011.06.033>.
- [44] R. Kurtaran, S. Odabaşoğlu, A. Azizoglu, H. Kara, O. Atakol, Experimental and computational study on [2, 6-bis (3, 5-dimethyl-N-pyrazolyl) pyridine]-[dithiocyanato] mercury (II), *Polyhedron* 26 (2007) 5069–5074, <https://doi.org/10.1016/j.poly.2007.07.021>.
- [45] I. Turel, L. Golić, P. Bukovec, M. Gubina, Antibacterial tests of bismuth (III)-quinolone (ciprofloxacin, cf) compounds against *Helicobacter pylori* and some other bacteria. Crystal structure of (cfH₂)₂ [Bi₂Cl₁₀]·4H₂O, *J. Inorg. Biochem.* 71 (1998) 53–60, [https://doi.org/10.1016/S0162-0134\(98\)10032-6](https://doi.org/10.1016/S0162-0134(98)10032-6).
- [46] M. Becka, M. Vilková, M. Šoral, I. Potočník, M. Breza, T. Bérés, J. Imrich, Synthesis and isomerization of acridine substituted 1, 3-thiazolidin-4-ones and 4-oxo-1, 3-thiazolidin-5-ylidene acetates. An experimental and computational study, *J. Mol. Struct.* 1154 (2018) 152–164, <https://doi.org/10.1016/j.molstruc.2017.10.046>.
- [47] I. Turel, P. Bukovec, M. Quiros, Crystal structure of ciprofloxacin hexahydrate and its characterization, *Int. J. Pharm.* 152 (1997) 59–65, [https://doi.org/10.1016/S0378-5173\(97\)04913-2](https://doi.org/10.1016/S0378-5173(97)04913-2).
- [48] E. Aktan, B. Babür, N. Seferoğlu, B. Çatukçaş, F.B. Kaynak, Z. Seferoğlu, Combined spectroscopic, XRD crystal structure and DFT studies on 2-(ethylthio) pyrimidine-4, 6-diamine, *J. Mol. Struct.* 1145 (2017) 152–159, <https://doi.org/10.1016/j.molstruc.2017.05.058>.
- [49] J.G. Haasnoot, Mononuclear, oligonuclear and polynuclear metal coordination compounds with 1, 2, 4-triazole derivatives as ligands, *Coord. Chem. Rev.* 200 (2000) 131–185, [https://doi.org/10.1016/S0010-8545\(00\)00266-6](https://doi.org/10.1016/S0010-8545(00)00266-6).
- [50] B.S. Holla, B.S. Rao, B. Sarojini, P. Akberali, One pot synthesis of thiazolidinopyrimidinones and evaluation of their anticancer activity, *Eur. J. Med. Chem.* 39 (2004) 777–783, <https://doi.org/10.1016/j.ejmech.2004.06.001>.
- [51] D. Seebach, Frontorbitale: Frontier Orbitals and Organic Chemical Reactions. Von I. Fleming. John Wiley & Sons, London 1976. 1. Aufl., V, 249 S., geh. § 3, 95, Wiley Online Library, 1977. <https://doi.org/10.1002/mad.19770250113>.
- [52] K. Krogmann, Die Kristallstruktur von K₂ [Pd (C₂O₄)₂]·4 H₂O, *Zeitschrift für anorganische und allgemeine Chemie* 346 (1966) 188–202, <https://doi.org/10.1002/zaac.19663460311>.
- [53] I. Ciofini, P.P. Lainé, F. Bedioui, C. Adamo, Photoinduced intramolecular electron transfer in ruthenium and osmium polyads: Insights from theory, *J. Am. Chem. Soc.* 126 (2004) 11182–11777, <https://doi.org/10.1021/ja0482278>.
- [54] I. Ciofini, C.A. Daul, C. Adamo, phototriggered linkage isomerization in ruthenium–dimethylsulfoxide complexes: insights from theory, *J. Phys. Chem. A* 107 (2003) 11182–11190, <https://doi.org/10.1021/jp0307607>.
- [55] M.E. Casida, Time-dependent density functional response theory for molecules, Recent Advances In Density Functional Methods: (Part I), World Scientific, 1995, pp. 155–192. https://doi.org/10.1142/9789812830586_0005.
- [56] R. Bauernschmitt, R. Ahlrichs, Treatment of electronic excitations within the adiabatic approximation of time dependent density functional theory, *Chem. Phys. Lett.* 256 (1996) 454–464, [https://doi.org/10.1016/0009-2614\(96\)00440-X](https://doi.org/10.1016/0009-2614(96)00440-X).
- [57] C. Litalien, P. Beaulieu, Molecular mechanisms of drug actions: From receptors to effectors, *Pediatric Critical Care, Elsevier* (2011) 1553–1568, <https://doi.org/10.1016/B978-0-323-07307-3.10117-X>.
- [58] N. Song, Y. Li, X. Sun, F. Qu, Synthesis of (+/-) ibuprofen sugar derivatives, *Yao xue xue bao = Acta pharmaceutica Sinica* 39 (2004) 105–109.
- [59] H.M. Faidallah, S.A. Rostom, Synthesis, anti-inflammatory activity, and COX-1/2 inhibition profile of some novel non-acidic polysubstituted pyrazoles and pyrano [2, 3-c] pyrazoles, *Arch. Pharm.* 350 (2017) 1700025, <https://doi.org/10.1002/ardp.201700025>.
- [60] A. Kumar, P. Lohan, D.K. Aneja, G.K. Gupta, D. Kaushik, O. Prakash, Design, synthesis, computational and biological evaluation of some new hydrazino derivatives of DHA and pyranopyrazoles, *Eur. J. Med. Chem.* 50 (2012) 81–89, <https://doi.org/10.1016/j.ejmech.2012.01.042>.

- [61] L.M. Zeldenryk, Occupational deprivation: a consequence of Australia's policy of assimilation, *Aust. Occup. Ther. J.* 53 (2006) 43–46, <https://doi.org/10.1111/j.1440-1746.2011.06980.x>.
- [62] Y. Gilgun-Sherki, Z. Rosenbaum, E. Melamed, D. Offen, Antioxidant therapy in acute central nervous system injury: current state, *Pharmacol. Rev.* 54 (2002) 271–284, <https://doi.org/10.1124/pr.54.2.271>.
- [63] P. Evans, Free radicals in brain metabolism and pathology, *Br. Med. Bull.* 49 (1993) 577–587, <https://doi.org/10.1093/oxfordjournals.bmb.a072632>.